Estuarine Muds Manual

E A Delo
M C Ockenden

Report SR 309
May 1992

HR Wallingford

Registered Office: HR Wallingford Ltd, Howbery Park, Wallingford, Oxfordshire OX10 8BA, UK
Telephone: 0491 35381 International + 44 491 35381 Telex: 848552 HRSWAL G.
Facsimile: 0491 32233 International + 44 491 32233 Registered in England No. 1622174

Contract

This report describes work funded by the Department of the Environment under Research Contract PECD 7/6/192 for which the nominated officer was Mr P Woodhead and by HR Wallingford. The HR job number was UQS 82. It is published on behalf of the Department of the Environment, but any opinions expressed in this report are not necessarily those of the Department of the Environment. The report was written by Dr E A Delo and Ms M C Ockenden.

Prepared by E.A Delo / M.C. Ockenden — Manager, Environmental Technology

Checked by E.A Delo — Manager, Environmental Technology

Approved by M.C. Ockenden — Project Manager

Date 29 June 1992

Summary

Estuarine Muds Manual

E A Delo
M C Ockenden

Report SR 309
May 1992

This report summarises, in an engineering form, the main processes of cohesive sediment behaviour, namely, deposition, consolidation and erosion. The data presented are intended to show the practising engineer which parameters are important in each of the processes and to enable broad estimates of the rates of deposition, consolidation and erosion to be made based on a limited knowledge of the field conditions.

The work was carried out as part of a strategic research programme on cohesive sediment transport processes undertaken for the Department of the Environment. This report extends and updates the first mud manual which was published in 1988 by incorporating the results of recent research undertaken by HR Wallingford, UK Universities and Polytechnics and international research groups.

The behaviour of cohesive sediment is controlled by a complex array of physical, chemical and biological factors, which are only partly understood. The usual methodology of engineering investigations which require a knowledge of the properties of cohesive sediment has been to determine either in-situ or in the laboratory the behaviour of the cohesive sediment. Accordingly, the data obtained is site specific. The properties of cohesive sediment will vary spatially within a site and to a greater extent will vary between sites. At present, it is not possible to predict the behaviour of a cohesive sediment from its physical and chemical properties alone.

The three processes of cohesive sediment of primary interest to the engineer are deposition, consolidation and erosion. Deposition involves the settling through the water column and on to the bed of flocculated sediment. Consolidation of a deposit is the gradual expulsion of interstitial water by the self weight of the sediment accompanied by an increase in both the density of the bed and its strength with time. Erosion is the removal of sediment from the surface of the bed due to the stress of the moving water above the bed.

The behaviour of cohesive sediment does vary considerably in quantitative terms from one source to another. Therefore, it is crucial that the engineer appreciates that estimates based on the data presented herewith may well be in error by half an order of magnitude. For large engineering problems involving cohesive sediment it would probably be essential to undertake a detailed study. This would involve most of the following techniques: field measurements, laboratory testing of sediment, modelling of hydrodynamics and sediment transport.

This controlled report is a commissioned subject area review which provides advice to practising engineers on the engineering properties of cohesive sediments. For further information please contact the Sediments Group.

Notation

A	=	semi-orbital excursion length = $U_m T/2\pi$ (m)
c	=	suspended sediment concentration (kgm^{-3})
c_b	=	near-bed suspended sediment concentration (kgm^{-3})
c_i	=	concentration of suspended sediment in class i (kgm^{-3})
c_o	=	constant sediment concentration of mud layer
$C_1 ... C_5$	=	consolidation constants in equations 3.1 and 3.2
$c(t)$	=	suspended sediment concentration as a function of time (kgm^{-3})
B_{wc}	=	constant determined by relative direction of waves and currents
d	=	water depth (m)
d_m	=	thickness of the fluidised layer (depth of fluid mud) (m)
dm/dt	=	rate of change of mass on the bed per unit area ($kgm^{-2}s^{-1}$)
d_{50}	=	median particle diameter (m)
E_1, E_2	=	constants in equation 4.1
f_c	=	current friction factor
f_w	=	wave friction factor = $\max(f_{wr}, f_{ws})$
f_{wr}	=	rough bed friction factor
f_{ws}	=	smooth bed friction factor
F	=	flocculation factor (w_s/w_{sd})
g	=	acceleration due to gravity (ms^{-2})
g_1, g_2	=	phase of tidal constituent at points 1, 2
H	=	wave height (m)
k	=	permeability (ms^{-1})
k	=	wave number $2\pi/L$ (m^{-1})
k_s	=	Nikuradse equivalent sand grain roughness (m)
K	=	constant in equation 2.1
L	=	wave length (m)
m_e	=	erosion constant ($kgN^{-1}s^{-1}$)
M	=	mass per unit area which is fluidised (kgm^{-2})
N	=	constant (in equation 2.1)
Q_m	=	sediment transport rate ($kgm^{-1}s^{-1}$)
r	=	relative roughness = A/k_s
R_1, R_2	=	tidal range at points 1, 2
Ri_B	=	bulk Richardson number
R_w	=	wave Reynolds number
t	=	time (s)
T	=	wave period (s)
u_*	=	shear velocity (ms^{-1})
u_m	=	mean velocity of fluid mud layer (ms^{-1})
U_b	=	bottom orbital velocity (ms^{-1})
U_m	=	maximum bottom orbital velocity (ms^{-1})
U	=	depth averaged current velocity (ms^{-1})
$U(y)$	=	velocity at height y (ms^{-1})
V_e	=	entrainment velocity (ms^{-1})
w_{50}	=	median settling velocity (ms^{-1})
w_s	=	flocculated settling velocity (ms_{-1})
w_{sd}	=	chemically dispersed settling velocity (ms_{-1})
w_{si}	=	settling velocity of sediment class i

Notation *(continued)*

δ	=	wave boundary layer thickness (m)
γ	=	shear rate (s^{-1})
κ	=	von Karman's constant (0.4)
η	=	water surface level relative to mean sea level (m)
θ	=	angle of bed slope
μ	=	dynamic viscosity of the mud (Nsm^{-2})
υ	=	kinematic viscosity (m^2s^{-1})
ρ_w	=	density of fluid (kgm^{-3})
ρ_b	=	bulk density of sediment (kgm^{-3})
ρ_d	=	dry density of sediment bed (kgm^{-3})
ρ_m	=	density of fluid mud layer (kgm^{-3})
ρ_o	=	formation density of bed (kgm^{-3})
σ_v'	=	vertical effective stress (Nm^{-2})
τ_0	=	shear stress at bottom of fluid mud
τ_i	=	shear stress at interface of mud and water
τ_b	=	applied bed shear stress (Nm^{-2})
τ_d	=	critical shear stress for deposition (Nm^{-2})
τ_{di}	=	critical shear stress for deposition of sediment class i (Nm^{-2})
τ_e	=	critical shear stress for erosion (Nm^{-2})
τ_m	=	peak bed shear stress (Nm^{-2})
$\tau(z)$	=	shear stress profile in the bed
ϕc_i	=	proportion of total concentration in sediment class i
ω	=	wave frequency $2\pi/T$ (s^{-1})
ω_{M2}	=	frequency of main M_2 tidal constituent

Contents

Contents (continued)

Contents *(continued)*

1 Introduction

1.1 General

This report summarises, in an engineering form, the main processes of cohesive sediment behaviour, namely, deposition, consolidation and erosion. The data presented are intended to show the practising engineer which parameters are important in each of the processes and to enable broad estimates of the rates of deposition, consolidation and erosion to be made based on a limited knowledge of the field conditions.

The work was carried out as part of a strategic research programme on cohesive sediment transport processes undertaken for the Department of the Environment. This report extends and updates the first mud manual which was published in 1988 by incorporating the results of recent research undertaken by HR Wallingford, UK Universities and Polytechnics and international research groups.

The aim of this report is to provide a means of dissemination of research findings on cohesive sediment to the practising engineer.

This report has five main chapters which are preceded by the next section which is an introduction to the cohesive sediment processes which explains the fundamental behaviour of cohesive sediment. Each of the main chapters is structured into sections each of which outline in summary form first the state of knowledge on the topic and then the procedure for making an engineering calculation. Chapter 2 describes the deposition process starting with flocculation and settling velocity, and moving on to deposition in still water and flowing water, fluid mud deposition and finally deposition under waves. Chapter 3 considers the consolidation processes with reference to the density variation in a cohesive bed with respect to depth and time. Chapter 4 presents a description of the erosion mechanisms for cohesive sediment including erosion by currents, fluidisation by waves, and movement and entrainment of a fluidised layer. Chapter 5 gives an outline of the rheological aspects of cohesive sediment by describing the flow behaviours. Chapter 6 describes the calculation of water surface slope and bed shear stress under currents and waves and in combination.

1.2 Cohesive sediment processes

The transport of cohesive sediment within estuarine or inland water courses creates a wide range of design, maintenance and management problems in ports, harbours and docks. Accumulation of sediment in navigation channels and berths often results in the need for expensive dredging operations. New developments require a sound engineering appraisal of the likely changes in the patterns of sediment movement which may result after the development. In addition, many pollutants are preferentially adsorbed on to the fine cohesive fraction of the sediment and hence, for ecological reasons, it is of great benefit to be able to predict the movement of the contaminated sediment.

The behaviour of cohesive sediment is controlled by a complex array of physical, chemical and biological factors, which are only partly understood. The usual methodology of engineering investigations which require a knowledge of the properties of cohesive sediment has been to determine either in-situ or in the laboratory the behaviour of the cohesive sediment. Accordingly, the data obtained is site specific. However, as the nature of

cohesive sediment is influenced by many processes, for example, deposition and consolidation history, wave disturbance, tidal current erosion, bioturbation, algal and organic inputs, the properties of cohesive sediment will vary spatially within a site and to a greater extent will vary between sites. At present, it is not possible to predict the behaviour of a cohesive sediment from its physical and chemical properties alone.

Estuarine cohesive sediment is composed primarily of silt and clay. For example, the size distributions of samples of cohesive sediments are given in Figure 1.1. Cohesive sediment contains a large proportion of very small particles which have a large specific area such that the effect of the surface physico-chemical forces becomes as important as the effect of gravity forces. Some of these individual particles are less than 1 micron in diameter and may be kept in suspension by Brownian motion alone. Flocculation of particles will take place when the net physico-chemical interparticle forces become attractive.

Flocculation of sediment particles is the consequence of particles sticking together as they are brought into contact with each other. Collision and cohesion are therefore the essential processes of flocculation and these factors are virtually independent of one another.

Cohesion is understood to be determined by the attractive forces of clay particles. These forces are strong at short distances, but fall rapidly with distance. Particles will cohere if these short range forces dominate the repulsive forces generated by the clouds of cations around the particles. The strength of the repulsive forces depends on the charge on the mineral surface, which is determined by the mineral composition, and by the amount and types of cations present in the suspending fluid.

Collisions of particles are the result of one of three mechanisms, namely, Brownian motion of suspended particles, internal shear of the water, and differential settling velocities of the particles or flocs. All three of these mechanisms operate in an estuary although it is considered that the formation of large aggregates is predominantly due to internal shearing.

Nevertheless, the size of flocs formed by collisions from any of the three mechanisms is limited by the maximum rate of internal shear that the flocs can withstand. It is evident, therefore, that internal shearing can both promote the growth of flocs and limit their size. Hence, suspended flocs should attain a maximum size given constant conditions of internal shear. The size and settling velocity of the flocs may be much larger than that of the individual particles.

Cohesive sediment can be considered to exist in four states. These four states are illustrated in Figure 1.2 (Ackers, 1988) and may be described as a mobile suspended sediment, a near bed stationary suspension of high concentration with a small cohesion which is sometimes referred to as fluid mud, a partially consolidated bed, and a settled bed. The three processes of cohesive sediment of primary interest to the engineer are deposition, consolidation and erosion. Deposition involves the settling through the water column and on to the bed. Consolidation of a deposit is the gradual expulsion of interstitial water by the self weight of the sediment accompanied by an increase in both the density of the bed and its strength with time. Erosion is the removal of sediment from the surface of the bed due to the stress of the moving water above the bed.

The behaviour of cohesive sediment does vary considerably in quantitative terms from one source to another and with time. Therefore, it is crucial that the engineer appreciates that estimates based on the data presented herewith may well be in error by half an order of magnitude.

For large engineering problems involving cohesive sediment it would probably be essential to undertake a detailed study. This would involve most of the following techniques: field measurements, laboratory testing of sediment, modelling of hydrodynamics and sediment transport.

2 Deposition

2.1 Flocculation and settling velocity

2.1.1 Knowledge

1. Flocculation of sediment particles is the consequence of particles sticking together as they are brought into contact with each other. Collision and cohesion are the essential processes of flocculation (Krone, 1962).

2. The size and hence the settling velocity of a floc will be much larger than that of the constituent individual particles. The data in Figure 2.1 shows the ratio of the settling velocities of flocculated and chemically dispersed discrete particles (Migniot, 1968). For particles of diameter 0.1 micron the ratio is 10,000. For a diameter of 60 microns there is little flocculation and the settling velocity ratio is 1. However, all estuarine sediments and suspended flocs have a range of constituent particle sizes and a simple settling velocity ratio does not exist.

3. The maximum floc size is governed by: the discrete particle sizes, suspended sediment concentration, mineralogy, organic content, Ph and ionic strength of the mud; the chemical composition of the pore water and suspending water; and the hydrodynamic parameters of the flow such as the velocity and turbulence structure, internal shear and bed shear stress.

4. The size distribution of flocs (aggregates of discrete particles) in the field has been studied (Krone, 1972) and directly measured using a submerged laser particle analyser (Bale and Morris, 1987), submerged video recording of settling through an open-ended column (van Leussen, 1988), and video image processing of settling in an Owen tube (Dearnaley, 1991).

5. Measurement of the settling velocity of flocculated sediment must be done in the field as removal of a sample to the laboratory changes the size distribution of the flocs. The data shown in Figure 2.2 indicates that laboratory measurements of median settling velocity could be an order of magnitude lower than those measured in the field with an Owen tube (Owen, 1971).

6. Each Owen tube measurement involves withdrawing samples from the tube over one hour, and during this time the presence of the tube itself has an impact on the settling velocity. Video image analysis of settling in an Owen tube has indicated that the median settling velocity determined by Owen tube analysis may underestimate the settling velocity particularly in the first 5-10 minutes of settling (Dearnaley, 1991).

7. A suspended cohesive sediment has a range of settling velocities due

to the size and density distributions of the flocs. A typical settling velocity distribution and median settling velocity of a concentration of 1kgm^{-3} of Thames suspended sediment is shown in Figure 2.3 (Stevenson and Burt, 1985). The median settling velocity w_{50} is the settling velocity for which half the sediment by weight will settle at a higher (or lower) velocity.

8. The median settling velocity of cohesive sediment is strongly dependent on the suspended sediment concentration. Median settling velocity w_{50} increases with increasing suspended sediment concentration c. The relationship may be approximated by the following empirical form of equation:

$$w_{50} = K c^N \quad \text{... (2.1)}$$

where K and N are constants.

9. The values of K and N vary considerably for different estuaries. A summary of results from Owen Tube experiments conducted by HR in nine estuaries which is shown graphically in Figure 2.4. The line drawn through the middle of the data can be represented by:

$$w_{50} = 0.001\ c^{1.0} \quad \text{... (2.2)}$$

10. Hindered settling is the process by which a high concentration of settling flocs interfere with their surrounding flow of fluid. It usually commences at a suspended sediment concentration of between 2kgm^{-3} to 10kgm^{-3} (Krone 1972, Burt and Stevenson 1983, Puls and Kuehl 1986). The settling velocity as a function of suspended concentration peaks and eventually decreases at very high suspended sediment concentrations. An example of settling velocity data for the Severn Estuary is given in Figure 2.5.

11. Changes in salinity above 2kgm^{-3} have only a small effect on the settling velocity of cohesive sediment (Burt and Stevenson, 1983).

2.1.2 Procedure

The settling velocity of a suspended cohesive sediment is often used in the form of Equation 2.1 in the prediction of the rate of deposition. Alternatively, the whole settling velocity distribution can be used to represent the differential settling of different sized aggregates.

New field measurements

1. Measure settling velocity distribution in the field using an Owen Tube or in-situ video for preferably at least 6 samples with a range of suspended sediment concentrations, and either

2. Use video image analysis to relate the settling velocity distribution to the floc size distribution and total concentration in suspension, or

3. For each sample, plot settling velocity against percentage by weight of sample exceeding that settling velocity and determine the median settling velocity w_{50} (similar to Figure 2.3), and

4. Plot median settling velocity w_{50} of each sample against suspended sediment concentration c on log scales and fit a straight line if appropriate (similar to a single line in Figure 2.4). Determine the values of K and N in Equation 2.1.

Existing field measurements

5. If the site of interest has been investigated before and the data is still appropriate use data in Figure 2.4.

No field measurements

6. Use Equation 2.2 (i.e. K = 0.001 and N = 1.0) with caution as there is a significant variation about this average relationship.

2.2 Deposition in still water

2.2.1 Knowledge

1. The rate of deposition of sediment to the bed can be described by the near-bed concentration of suspended sediment c_b and its median settling velocity w_{50}. In still water, the rate of deposition of sediment from suspension dm/dt can be expressed by:

$$dm/dt = - c_b w_{50} \quad \text{... (2.3)}$$

2. The concentration of suspended sediment will decrease with time as sediment deposits on the bed and the rate of deposition will accordingly decrease.

3. There is likely to be a gradient of concentration of suspended sediment in the water column with the near-bed concentration greater than the depth-mean average.

2.2.2 Procedure

New field measurements

1. The instantaneous rate of deposition can be calculated from the measured median settling velocity relationship and the near-bed suspended sediment concentration with Equation 2.3.

Existing field measurements

2. If the site of interest has been investigated before and the data is still appropriate look up the rate of deposition given in Figure 2.4 for the respective estuary.

No field measurements

3. Use the average settling velocity relationship given in Equation 2.2 with caution and the near-bed suspended sediment concentration with Equation 2.3.

2.3 Deposition in flowing water

2.3.1 Knowledge

1. Laboratory tests have been conducted in straight and circular flumes to investigate the mechanism of deposition of cohesive sediment (Krone 1962, Partheniades 1962, Postma 1962, Partheniades et al. 1966, Partheniades et al. 1968, Mehta and Partheniades 1973, Mehta 1988, Kusuda et al. 1982, Burt et al. 1985, Delo 1988).

2. Field measurement of the deposition of cohesive sediments in estuaries during single tides has been undertaken recently by HR Wallingford (Diserens, Delo and Ockenden, 1991). The hydrodynamics of the flow (including wave

induced currents), suspended sediment concentration and the bed elevation were recorded.

3. The rate of deposition of cohesive sediment from suspension dm/dt can be modelled by the near-bed concentration c_b, median settling velocity w_{50}, bed shear stress τ_b exerted by the flowing water and a critical bed shear stress τ_d, which is defined as the bed stress above which there is no deposition of suspended sediment. For a uniform sediment, or one for which the settling velocity is approximated by the median settling velocity, an empirical equation can be used to calculate the rate of deposition:

$$dm/dt = -(1 - \tau_b/\tau_d)\, c_b\, w_{50} \quad \text{for } \tau_b < \tau_d \qquad \ldots (2.5)$$

4. The critical bed shear stress for deposition of cohesive sediment τ_d, is estimated from laboratory tests to be between $0.06 Nm^{-2}$ and $0.10 Nm^{-2}$.

5. Suspended cohesive sediments can be considered to consist of flocs which have a distribution of sizes, densities, settling velocities, strengths and critical shear stresses for deposition. The representation of these suspended sediments at a particular concentration by a median settling velocity and a single critical shear stress for deposition of all the sediment is therefore an approximation. Part of the suspended sediment will deposit at bed shear stresses greater than the 'average' critical stress given above. Figure 2.6 shows the fraction of sediment remaining in suspension following deposition in flowing water. The deposition of a distributed suspended cohesive sediment has been investigated and modelled (Mehta 1988, Mehta and Lott 1987, Delo 1988, Krishnappen 1991, Verbeek et al 1991, Ockenden and Williamson 1992), but the approach requires more input information than for a uniform sediment.

6. A distributed sediment can be modelled by dividing the sediment into classes, each with a unique settling velocity, w_{si}, concentration, c_i, and critical shear stress for deposition, τ_{di}. The total sediment deposited on the bed, Δm, during a time interval, Δt, is given by the sum of the individual amounts deposited from each class:

$$\Delta m = \sum_{1}^{N} w_{si}\, \phi c_i\, c(t)\, (1 - \tau_b/\tau_{di})\, \Delta t \qquad \ldots (2.6)$$

where

ϕc_i = proportion of the total concentration in sediment class i
$c(t)$ = suspeneded sediment concentration at time t

Sediment class i only deposits if $\tau_b \leq \tau_{di}$.

2.3.2 *Procedure*

New field and laboratory measurements

1. The instantaneous rate of deposition can be calculated from the measured median settling velocity relationship, the near-bed suspended sediment concentration, the shear stress at the bed and an assumed value of τ_d ($0.08 Nm^{-2}$) with Equation 2.5.

2. A field bed frame can be deployed to measure the hydrodynamics, suspended sediment concentration and bed elevation through a tide. The data can be used to determine the in-situ rate of deposition. In addition, a validated deposition algorithm similar to that given by Equation 2.5 can be evaluated.

3. Use video image analysis or similar equipment to make measurements of the settling velocity distribution and floc size distribution. Use this to model deposition of distributed sediment according to Equation 2.6.

4. Determine the critical shear stress for deposition (single value or value for each sediment band) from laboratory deposition tests in a straight or annular flume.

Existing field measurements

5. If the site of interest has been investigated before and the data is still appropriate use the settling velocity from Figure 2.4 and use Equation 2.5 with an assumed value of τ_d ($0.08 Nm^{-2}$) to calculate the instantaneous rate of deposition of suspended cohesive sediment from flowing water.

No field measurements

6. Use with caution the average settling velocity relationship (Equation 2.2) and Figure 2.4 with an assumed value of τ_d ($0.08 Nm^{-2}$) to calculate the instantaneous rate of deposition suspended cohesive sediment from flowing water.

7. Estimate the shear stress for deposition for each class of a distributed sediment from Figure 2.5.

2.4 Fluid mud

2.4.1 Knowledge

1. Fluid mud may be formed by settlement from a mud suspension in either still or flowing water, or by disturbance of a settled bed by wave action (see section 4.2) or mechanical agitation.

2. The settling velocity reaches a peak of approximately 2 - $4 mms^{-1}$ and remains constant for suspended sediment concentrations in the range $4 kgm^{-3}$ to $20 kgm^{-3}$. The flocs hinder the displacement of the water as they settle. However, although the flocs touch each other, they are too weak to transmit significant forces without deforming. The settling velocity decreases rapidly as the suspended sediment concentration increases above $20 kgm^{-3}$ and may typically be $0.05 mms^{-1}$ at $75 kgm^{-3}$ (see Figure 2.5).

3. In the absence of a significant amount of vertical turbulent exchange near slack water, the net flux of settling particles is the product of the settling velocity and the concentration of mud in suspension near the bed. This flux rises to a maximum of around $40 gm^{-2}s^{-1}$ at a suspended sediment concentration of approximately $20 kgm^{-3}$ and reduces at higher suspended sediment concentrations as shown in Figure 2.7. Fluid mud with a suspended sediment concentration of $70 kgm^{-3}$ dewaters or deposits onto the bed typically at a rate of about $0.004 kgm^{-2}s^{-1}$.

4. A layer of fluid mud above the bed will only grow in thickness if the flux of mud settling on to the bed exceeds the rate at which the fluid mud dewaters to become a weak soil. This is equivalent to a suspended sediment concentration of approximately $2.5 kgm^{-3}$ in the overlying water.

5. Fluid mud with suspended sediment concentrations of $70 kgm^{-3}$ to $100 kgm^{-3}$ have been reported in the Parrett (HR, 1991), Severn (Kirby and Parker, 1973), Weser (Wellershans, 1981), Gironde (Barbier, 1977), Thames (Odd and Owen, 1972) and other places around the world.

6. If the shear stress between a moving fluid mud layer and the bed falls below $0.1Nm^{-2}$ it will de-water. Fluid mud dewaters at a rate of approximately $0.05mms^{-1}$ to form a weak soil with a dry density of $100kgm^{-3}$ to $300kgm^{-3}$ which does not flow easily (HR, 1991).

2.4.2 Procedure

Field and laboratory measurements

1. Measure suspended sediment concentrations by sampling or optical techniques. If the suspended sediment concentration is greater than $2.5kgm^{-3}$ preceding slack water, fluid mud is likely to be formed.

2. Measure dewatering rates in the field using echo sounding techniques to record the fluid mud/water interface, or

3. Conduct laboratory tests on fluid mud pumped out of the field to determine dewatering rates.

No field measurements

3. Calculate the flux of settling mud to the bed according to Figure 2.7.

4. Assume a constant dewatering rate of $0.05mms^{-1}$.

2.5 Deposition in waves

2.5.1 Knowledge

1. Surface waves generate orbital velocities and an oscillating shear stress on the bed. The wave induced bed shear stress will augment the current induced bed shear stress. The deposition of cohesive sediment could be prevented by wave action particularly in shallow waters.

2.5.2 Procedure

1. From a knowledge of the wave climate calculate the frequency distribution of wave induced peak bed shear stress. Compare this with the current induced bed shear stresses and the value of the critical stress for deposition τ_d to compute the rate of deposition.

3 Consolidation

3.1 Density variation with depth and time

3.1.1 Knowledge

1. There is a lack of knowledge regarding the interface between a flowing suspended sediment and a deposited bed. This is due primarily to the difficulty in measuring flow and suspended sediment concentration at the necessary resolution (less than 10mm) to define the physics close to the bed.

2. However, from laboratory studies it may be assumed that the sediment deposited to the bed has an initial formation dry density ρ_o of approximately $30\text{-}70kgm^{-3}$.

3. The deposited cohesive sediment of the bed will consolidate under its self weight. This process comprises the expulsion of the pore water with

accompanying large strains. The excess pore pressures within the cohesive bed will dissipate with time and the interparticle stress σ_v' will increase. The floc matrix will compress to form a structure of higher density ρ_d with a correspondingly lower permeability k.

4. The consolidation process for a cohesive sediment bed will generally result in a density profile which increases with depth below the surface and with time.

5. The density at any point and time within a cohesive sediment bed will depend to a large degree on the time history of the deposition to the bed and the physical characteristics of the cohesive sediment.

6. The vertical effective stress σ_v' is the interparticle stress and is given by the difference between the total stress and the pore water pressure.

7. Two empirical relationships have been derived from laboratory tests in consolidation columns on cohesive sediments. However, even for the same type of cohesive sediment the relationships are dependent on the rate and quantity of deposition. The effective stress σ_v' can be expressed as a function of dry density ρ_d (a typical relationship is shown in Figure 3.1) by

$$\sigma_v' = C_1 + C_2 \rho_d + C_3 \rho_d^2 \quad \text{... (3.1)}$$

The permeability k of the cohesive sediment can also be expressed as a function of dry density ρ_d (Figure 3.2) by

$$\log(k) = C_4 + C_5 \rho_d \quad \text{... (3.2)}$$

where C_1 ... C_5 are constants.

Both relationships describe consolidation after the first few hours. In the early stages of consolidation, these relationships appear to show some dependency on time.

8. To predict the density at a given time and depth within a cohesive sediment bed requires a knowledge of the time history of the deposition to, and erosion from the bed, the formation density of deposits and the empirical relationships between effective stress and dry density, and permeability and dry density.

9. The density structure of cohesive sediment beds vary considerably between sites and at any particular site. In a navigation channel experiencing net deposition, the dry density could increase from 200kgm^{-3} near the surface to 500kgm^{-3} at a depth of 1m. An inter-tidal mudflat however is likely to have a near surface dry density of approximately 500kgm^{-3} (ie. below any recent deposits) and a dry density of approximately 1000kgm^{-3} at a depth of 1m. A sub-tidal cohesive sediment bed which does not experience significant net deposition is likely to have a density structure similar to an inter-tidal mudflat.

3.1.2 Procedure

Field and laboratory measurements

1. Obtain in-situ measurement of density in the upper 1m of the cohesive sediment bed at the site of interest using an instrument such as a Harwell gamma ray density probe.

2. Conduct consolidation column tests by depositing a cohesive sediment bed from a suspension at an appropriate rate, and measure density and permeability. Determine the values of the constants in Equations 3.1 and 3.2 and the formation density.

3. If cohesive sediment from the site has been previously tested in the laboratory use the empirical relationships given.

4. Run a mathematical model to predict the density with time and depth using the laboratory derived relationships. Compare model results with the existing conditions from in-situ measurements.

No field measurements

1. Use the empirical relationships below with caution to run a mathematical model to predict the density with time and depth.

$$\rho_o = 50 kgm^{-3} \quad \text{... (3.3)}$$

$$\sigma_v' = C_1 + C_2 \rho_d + C_3 \rho_d^2 \quad \text{... (3.1)}$$

$$\log(k) = C_4 + C_5 \rho_d \quad \text{... (3.2)}$$

4 Erosion

4.1 Erosion by currents

4.1.1 Knowledge

1. The flocs on the surface of a cohesive sediment bed are bound together by interparticle attractive forces. To remove a floc by flowing water requires a shear stress sufficient to overcome the attractive forces. The erosion shear strength of a cohesive sediment surface is defined as the shear stress required to be exerted by the flowing water to cause erosion of flocs.

2. The erosion shear strength τ_e of a cohesive sediment bed has been shown by laboratory studies (HR Wallingford, 1989) to be related to the dry density ρ_d by the following form of empirical equation

$$\tau_e = E_1 \rho_d^{E2} \quad \text{... (4.1)}$$

3. The erosion shear strength of a cohesive sediment bed usually increases with depth together with the dry density. Therefore, under a constant fluid bed shear stress τ_b an eroding cohesive sediment bed will eventually cease to erode when the erosion strength of the exposed cohesive sediment τ_e is equivalent to τ_b (Figure 4.1).

4. At shear stresses well in excess of the critical floc erosion shear strength, a cohesive sediment bed may experience mass erosion. The process of mass erosion comprises the detachment of lumps of cohesive sediment from the bed. There is little quantitative field or experimental data on the mass erosion of cohesive sediment.

5. The rate of erosion of cohesive sediment has been studied in laboratory flume experiments (HR Wallingford, 1989) and to a lesser extent in the field

(Diserens et al, 1991). It has been found that the rate of erosion dm/dt is related to the magnitude of the excess shear stress ($\tau_b - \tau_e$) by the constant m_e. This can be expressed by the empirical equation:

$$dm/dt = m_e (\tau_b - \tau_e) \text{ for } \tau_b > \tau_e \quad \ldots (4.2)$$

6. There is considerable variation in the erosion properties of cohesive sediments from different sites. The average and range of erosion properties of cohesive sediments tested at HR Wallingford are presented in Figures 4.2 and 4.3.

4.1.2 Procedure

Field and laboratory measurements

1. If a suitable field erosion device exists for the site of interest, make in-situ measurements of the surface erosion strength, dry density and rate of erosion and determine the variation of erosion strength and density with depth below the surface, or

2. Obtain a sample of cohesive sediment from the site and investigate its erosional properties in a laboratory flume. Derive the values of the constants in Equations 4.1 and 4.2 from the experimental results.

Existing field or laboratory measurements

4. If the site of interest has been investigated in the past by field or laboratory experiments and the results are still appropriate use those values.

No field or laboratory measurements

5. Use with caution the average values of the erosion constants for Equations 4.1 and 4.2 shown in Figures 4.2 and 4.3.

4.2 Fluidisation by waves

4.2.1 Knowledge

1. Under cyclic loading by waves, the structure of the bed may be progressively weakened. The mud bed responds in both an elastic and a viscous manner; the elastic response is in the form of a restoring force (restoring the bed to its undisturbed position) while the viscous response is in the form of a dissipative force. Eventually, there is a complete breakdown of the structure (fluidisation), which allows the mud bed to be eroded or entrained much more easily.

2. The damping of waves over a fluid mud bed, showing the dissipation of wave energy, has been observed in flumes and in the laboratory. Hence, the estimation of shear stress at the bed surface for the purpose of correlation with the rate of erosion should not necessarily be based on the assumption of a rigid bed (Maa and Mehta, 1985).

3. Fluidisation of the mud is dependent on the wave characteristics and the mud properties (Derbyshire and Kendrick, 1987).

4. The action of the waves may be sufficient to cause surface erosion, with material passing directly into suspension. Experiments with a natural mud bed have shown that wave action erodes mud of a given dry density at about the same peak shear stress as that required with uni-directional flow. The erosion

rate was found to be similar to the proportional excess shear stress relationship for current erosion given in Equation 4.2 (Diserens and Delo, 1988).

5. A very high proportion of the eroded mud is contained within the relatively thin wave boundary layer because the sharp density gradient damps the vertical turbulent exchange with the water column above. The vertical turbulent exchange increases as the flow velocity of the overlying water increases.

4.2.2 Procedure

Laboratory measurements

1. Conduct laboratory tests under combined waves and currents to determine a critical wave shear stress for fluid mud generation and movement or entrainment into suspension.

No field or laboratory measurements

2. Calculate the combined wave and current shear stress from the current velocities and wave conditions (Equation 6.13).

3. Calculate the mass which is fluidised, M, by assuming that the bed is fluidised to a depth (and density) at which the shear strength of the bed (Figure 4.2) is equal to the combined wave and current shear stress. Assume that the fluidised material is contained within a thin layer close to the bed. Calculate the thickness of the layer, d_m, according to:

$$d_m = \max(M/0.075, \delta) \quad \text{... (4.3)}$$

where

d_m = thickness of the fluidised layer (m)
M = mass per unit area which is fluidised (kgm^{-2})
δ = wave boundary layer thickness
$= (f_w/2)^{0.5} U_b T/4\pi$
f_w = wave friction factor
U_b = bottom orbital velocity (ms^{-1})
T = wave period (s)

The wave friction factor and bottom orbital velocity can be calculated according to the procedure in section 6.3.

4.3 Movement of fluidised layer

4.3.1 Knowledge

1. Once the mud has been fluidised it will move more easily than a structured bed. It may flow under forces due to a sloping bed, the water surface slope or the mud/water interface slope. It may also be entrained into the overlying water.

2. The effects of the bed slope or the water surface slope are generally much more significant than the effect of the interface slope between the fluid mud and the overlying water, unless the interface slope is the only forcing factor (eg open water dumping of mud over a flat bed).

3. Field observations (HR Wallingford, 1991) have not shown any indication of a significant shear stress below which the fluid mud did not move.

However, there was a strong tendency for the fluid mud to dewater and consolidate with low bed stresses in the order of 0.1Nm^{-2}. Measured velocity profiles in the fluid mud layer could be predicted by application of a smooth turbulent theory, allowing a thick laminar sub-layer (in which viscous forces predominate) and a smooth turbulent region with a logarithmic velocity profile.

4. For fluid mud moving down a bed slope, the ratio of the shear stress at the interface between the water and mud, τ_i, to the shear stress at the bed, τ_0, is approximately 0.43 (Harleman, 1961).

5. For fluid mud moving under a water surface slope, the ratio of the shear stress at the interface, τ_i, to the shear stress at the bed, τ_0, is a function of the water depth:

$$\tau_i = \tau_0 (1 - d_m/d) \quad \text{... (4.4)}$$

where

τ_0 = shear stress at bottom of fluid mud
τ_i = shear stress at interface of mud and water
d_m = depth of fluid mud
d = depth of overlying water

4.3.2 Procedure

Field measurements

1. Use field equipment to the measure the velocity profile in the fluid mud layer and overlying water column during formation and movement of the fluid mud layer.

No field measurements

2. If the mud is on a slope, use the depth of the fluid mud layer to calculate the velocity of the layer due to the bed slope from Figure 4.4. This figure has been calculated assuming that smooth turbulent theory applies in the fluid mud layer. It assumes a uniform density for the fluid mud layer of 1075kgm^{-3}, and a uniform dynamic viscosity of 0.7Nsm^{-2}.

3. If the layer is subject to a water surface slope, calculate the water surface slope according to section 6.1. Calculate the velocity of the layer moving due to this water surface slope from Figure 4.5.

4. Calculate the sediment transport rate, Q_m, according to:

$$Q_m = \rho_m d_m u_m \quad \text{... (4.5)}$$

4.4 Entrainment of a fluidised layer

4.4.1 Knowledge

1. The entrainment of clear water into a fluid mud layer appears to behave in a similar way to the mixing of a salt wedge. Entrainment occurs if the bulk Richardson number, Ri_B, is lower than about 10. The entrainment velocity varies as a function of Ri_B (HR, 1991).

2. The bulk Richardson number Ri_B is:

$$Ri_B = \Delta\rho\ g\ d_m / \Delta u^2 \quad \text{... (4.6)}$$

where

$\Delta\rho$ = density difference between fluid mud and water
Δu = the difference between the fluid mud velocity and the overlying water velocity.

3. The entrainment rate may be approximated to that of a salt wedge:

$$dm/dt = -V_e\ \Delta u\ c_o,\ Ri_B < 10 \quad \text{... (4.7)}$$

where

$$V_e = u_m \frac{0.1}{(1+63Ri_B^2)^{0.75}} \quad \text{... (4.8)}$$

c_o = constant sediment concentration of mud layer

4.4.2 Procedure

1. Calculate the bulk Richardson number according to Equation 4.6. If $Ri_B \leq 10$, calculate entrainment rate according to Equations 4.7 and 4.8, or

2. Use Figures 4.4 and 4.5 to estimate whether mud is entrained given the depth and velocity of the layer.

4.5 Movement of a viscous layer

4.5.1 Knowledge

1. Even quite dense (>200kgm^{-3}) deposits of mud can move with time, with the rate of spreading much too slow to be described by the movement of fluid mud. The mud can be described theoretically as a viscous layer of thickness h moving down a slope of angle θ. For viscous flow, with constant viscosity

$$\tau(z) = \mu\ dU/dz \quad \text{... (4.9)}$$

where

$\tau(z)$ = shear stress at height z in the bed
μ = dynamic viscosity of the mud (Nsm^{-2})
$U(z)$ = velocity at height z in the bed

4.5.2 Procedure

1. Assume a constant density and constant viscosity (reasonable for a thin layer). Calculate the force balance:

$$(\rho_b - \rho_w)\ g\ \sin\theta + d\tau/dz = 0 \quad \text{... (4.10)}$$

2. Assume a no-slip condition at the bottom of the layer. Then the velocity profile in the layer is :

$$U(z) = (\rho_b - \rho_w)\ g\ \sin\theta\ (hz - 0.5z^2) / \mu \quad \text{... (4.11)}$$

3. Use a density in the range 150 - 300 kgm^{-3}

4. Use a viscosity in the range 0.2 - 0.7 Nsm^{-2}

5 Rheology

5.1 Flow behaviour

5.1.1 Knowledge

1. The rheological behaviour of cohesive sediments is strongly influenced by physico-chemical factors such as salinity, pH, mineralogical composition, solid particle properties and organic matter. This influence is largely reflected in the way in which these factors affect the flocculation process (Bryant, James and Williams, 1980; Verreet and Berlamont, 1988; James and Williams, 1982).

2. Several different rheological models have been used to describe cohesive sediment. These models are given in Table 5.1, with a schematic representation of the flow curves given in Figure 5.1 (after Verreet and Berlamont, 1987). Deviation from Newtonian behaviour occurs at a concentration of around 10kgm^{-3} dry density. In a shear-thinning material, the apparent viscosity decreases with increasing shear rate. A visco-elastic material has properties of liquids (dissipation of viscous energy by means of flow) and of solids (storage of elastic energy). Thixotropy is shown by a hysteresis loop for increasing or decreasing shear rate: there is no longer unique relation between shear stress, τ, and shear rate, γ.

3. Most mud type suspensions exhibit Newtonian type behaviour at low concentrations but show non-Newtonian shear-thinning or thixotropic viscoelastic behaviour at higher concentrations. The transition from shear-thinning to viscoelastic properties takes place over a range of only a few percent of the solids volume fraction of the suspension.

4. It is important to be able to define the flow regime exactly since approximations in calculations of shear stress and shear rate can lead to significant errors in prediction of low parameters such as apparent viscosity and yield stress.

5. Only equilibrium flow curves are capable of being analysed in a meaningful manner for time dependent non-Newtonian materials. The presence of an apparent yield stress indicates that the upper limiting solids concentration for successful application of steady shear techniques has been reached (Williams and Williams, 1989).

6. A controlled stress rheometer differs from a controlled shear rate instrument in that a shear stress is applied to the sample to be measured. This enables more meaningful low shear data to be produced since the instrument reacts in 'sympathy' to the fluid behaviour and does not force the material to move as in a controlled shear rate apparatus. Several researchers have published studies of direct yield measurements (James, Williams and Williams, 1987). Relationships between rigidity modulus, yield stress and volume fraction of cohesive sediment and concentrated suspensions of Na-illite (a model sediment) have been published by Williams and Williams (1989, 1990).

7. For low concentrations it is generally recognised that if careful experiments are carried out at very low shear rates then whatever the stress applied the material will flow (no yield stress) but it is all a matter of time scale (Bryant, James and Williams, 1980; Jones and Golden, 1990). For a particular shear rate the shear stress increases with increase in concentration. However, the concept of yield stress is dependent on the time of the experiment. In certain flow situations the existence of a yield stress can prove to be very useful, with correlations with various physical properties.

8. The Bingham model adequately represents the shear stress/shear rate relationship. The non-Newtonian fluid properties of the mixtures are largely functions of the concentration and the type of clay in the fluid matrix. The apparent viscosity and Bingham yield stress depend on the shear rate and increase exponentially with sediment concentration (O'Brien and Julien, 1986; Jones and Golden, 1990). The yield stress and viscosity can increase by three orders of magnitude as the volume concentration of sediment changes from 10-40% (O'Brien and Julien, 1988).

5.1.2 Procedure

Field and laboratory measurements

1. Use in-situ rheometers to measure the response of a cohesive sediment bed to shear.

2. Determine the shear stress/shear rate curve for a sample of material in a laboratory rheometer. This should be a controlled stress rheometer which does not force the material to move. Test at low shear rates (< 1/s).

No field or laboratory measurements

3. Use the flow curve presented in Figure 5.2 to determine an approximate shear stress/shear rate response for a given concentration. These curves relate to the "up curve"; ie conditions for the start-up of flow.

6 Water surface slope and bed shear stress

6.1 Water surface slope

6.1.1 Knowledge

1. The water surface slope at a point in a UK estuary can be estimated from the tidal range at two points 5-10km upstream and downstream of the site and from the 'g' phase of the main M_2 tidal constituent (at the same two sites), which is listed in the back of tide tables. The water surface slope is calculated from the difference in the water levels at the upstream and downstream locations, x km apart:

$$\partial\eta/\partial x = \{ \tfrac{1}{2} R_1 \cos(\omega_{M2}t - g_1) - \tfrac{1}{2} R_2 \cos(\omega_{M2}t - g_2) \} / x \quad \ldots (6.1)$$

where

R_1, R_2 = tidal range at points 1, 2

g_1, g_2 = phase of tidal constituent at points 1, 2

ω_{M2} = frequency of main M_2 tidal constituent

t = time

6.1.2 Procedure

1. Calculate the water surface slope according to Equation 6.1. If using the water surface slope for estimation of movement of fluid mud, calculate the maximum surface slope over the time period in the tide where fluid mud is expected, or

2. Use tide tables to predict the complete tide curve at both the upstream and downstream sites, relative to mean sea level. Calculate the water surface slope from the difference in water levels.

6.2 Currents

6.2.1 Knowledge

1. The shear stress generated at the bed by currents can be obtained from direct field measurement or estimated by a knowledge of the bed roughness, flow depth and mean current, although extra care is need in stratified flows.

6.2.2 Procedure

1. Measure the mean current speed and direction at 3 to 5 heights above the bed within the lower 1m of flow every half hour through a tidal cycle. Plot speed U(y) against the natural logarithm of height above bed $\log_e(y)$ for each set of measurements. Fit a straight line and determine its gradient. Calculate the shear velocity u_* from the equation:

$$U(y) = u_*/\kappa \log_e(y) + \text{constant} \qquad \ldots (6.2)$$

The value of von Karman's constant κ is 0.4.

2. Or, use a single mean current speed at a height above the bed y or the depth averaged mean current speed U(assume y=0.4 times water depth) and the smooth turbulent law given by:

$$U/u_* = 1/\kappa \log_e(u_* y/\nu) + 5.5 \qquad \ldots (6.3)$$

in which the value of κ is 0.4 and ν is the kinematic viscosity of water ($\approx 10^{-6}$).

3. The bed shear stress τ_b is given from the shear velocity by:

$$\tau_b = \rho_w u_*^2 \qquad \ldots (6.4)$$

in which ρ_w is the density of the water.

4. Or, measure the turbulent fluctuating current speeds in three orthogonal directions at preferably two heights above the bed within the lower 1m of flow. Determine the shear stress from the turbulent kinetic energy and Reynolds stress methods (Soulsby and Humphrey, 1989).

6.3 Waves

6.3.1 Knowledge

1. The shear stress generated at the bed by waves can be obtained by direct field measurement or estimated by a knowledge of the bed roughness, flow depth, wave height, period and length.

2. Techniques for calculating the peak orbital velocities are well described elsewhere (Soulsby and Smallman, 1986).

3. For given values of wave height and period, and depth of water, the maximum bottom orbital velocity can be calculated using first order linear wave theory from the relationship

$$U_m = \frac{\pi H}{T \sinh (2\pi d/L)} \qquad \text{... (6.5)}$$

where

U_m = maximum bottom orbital velocity (ms^{-1})
H = wave height (m)
T = wave period (s)
d = water depth (m)
L = wave length (m)

The magnitude of the wave length is determined iteratively, since

$$\omega^2 = gk \tanh (kd) \qquad \text{... (6.6)}$$

where

$\omega = 2\pi/T$ (s^{-1})
g = acceleration due to gravity (ms^{-2})
$k = 2\pi/L$ (m^{-1})

- the peak bed shear stress under a wave can be calculated from

$$\tau_m = \tfrac{1}{2}\rho_w f_w U_m^2 \qquad \text{... (6.7)}$$

where

τ_m = peak bed shear stress (Nm^{-2})
ρ_w = fluid density (kgm^{-3})
f_w = wave friction factor
U_m = maximum bottom orbital velocity

- the wave friction factor is dependent on the wave Reynolds number and the relative roughness, ie

$$R_w = \frac{U_m A}{\upsilon} \qquad \text{... (6.8)}$$

where

R_w = wave Reynolds number
U_m = maximum bottom orbital velocity (ms^{-1})
A = semi-orbital excursion length = $U_m T/2\pi$ = (m)
υ = kinematic viscosity (m^2s^{-1})

and

$$r = \frac{A}{k_s} \quad \text{... (6.9)}$$

where

r = relative roughness
A = semi-orbital excursion length = $U_m T/2\pi$ (m)
k_s = Nikuradse equivalent sand grain roughness (m)

6.3.2 Procedure

Field measurements

1. Record record water pressure fluctuations or water surface profile and use established techniques to derive wave height, wave period and depth of water or record turbulent oscillating currents within 1m above the bed.

2. The maximum bottom orbital velocity can be calculated using Equation 6.5 or obtained from a general curve (Soulsby and Smallman, 1986) given in Figure 6.1.

3. The peak bed shear stress can be calculated using Equation 6.7 with f_w being the greater of the smooth (laminar or smooth turbulent) and rough bed friction factors.

4. The smooth bed friction factor is calculated from

$$f_{ws} = B\ R_w^{-N} \quad \text{... (6.10)}$$

where

f_{ws} = smooth bed friction factor
R_w = wave Reynolds number

and for $R_w \leq 5.10^5$ (laminar)

$B = 2$
$N = 0.5$

or for $R_w \geq 5.10^5$ (smooth turbulent)

$B = 0.0521$
$N = 0.187$

- the rough bed friction factor is calculated from

$$f_{wr} = 0.3 \text{ if } A/k_s \leq 1.57 \quad \text{... (6.11)}$$

or

$$f_{wr} = 0.00251 \exp[5.21 (\frac{A}{k_s})^{-0.19}] \text{ if} A/k_s \geq 1.57 \quad \text{... (6.12)}$$

where

f_{wr} = rough bed friction factor
A = semi-orbital excursion length = $U_m T/2\pi$ (m)
k_s = Nikuradse equivalent sand grain roughness (m)

6.4 Combined wave and current shear stress

6.4.1 Knowledge

1. The combined effect of the waves and currents depends on the relative direction of the waves and currents. According to Soulsby (1991), the combined shear stress can be calculated according to:

$$\tau_b = 0.125 f_c \rho U^2 + 0.5 f_w \rho U_b^2 + \rho B_{wc} (f_c f_w/2)^{-0.5} U_m |U| \quad \text{... (6.13)}$$

where

f_c = current friction factor
B_{wc} depends on the relative direction of the waves and currents.

6.4.2 Procedure

1. Use laboratory or field data under combined waves and currents to calculate a value of B_{wc} for the required direction, or

2. If relative direction is unknown, calculate the combined wave/current shear stress including an interaction term according to Equation 6.13, using B_{wc}=0.36.

7 References

Ackers P. Personal communication January 1988.

Bale A J, Morris A W, 1987. In situ measurements of particle size in estuarine waters. Estuarine, Coastal and Shelf Science, Vol 24, pp253-263.

Barbier J M, 1977. Study of the mechanism of mud movement in the Gironde. 24th Int. Navigation Congress. Leningrad, 1977.

Bryant R, James A E, and Williams D J A, 1980. Rheology of Cohesive Sediments Industrialised Embayments and their Environmental Problems. Collins.

Burt T N and Game A C, 1985. Deposition of fine sediment from flowing water: An investigation of dependence on concentration, Hydraulics Research Ltd, Wallingford, UK. Report No SR 27.

Burt T N and Stevenson J R, 1983. Field settling velocity of Thames mud, Hydraulics Research Ltd, Wallingford, UK. Report No IT 251.

Dearnaley M P, 1991. Flocculation and settling of cohesive sediments. HR Wallingford, Report SR 272.

Delo E A, 1988. Deposition of cohesive sediment from flowing water, Hydraulics Research Ltd, Wallingford, UK. Report No SR 152.

Derbyshire B V and Kendrick M, 1987. Laboratory experiments on a near-bed turbid layer, Hydraulics Research Ltd, Wallingford, UK. Report SR 88.

Diserens A P and Delo E A, 1988. The stability of cohesive dredged slopes under wave action, Hydraulics Research Ltd, Wallingford, UK. Report SR 154.

Diserens A P, Delo E A, Ockenden M C, 1991. Estuarine sediments - near-bed processes: Field measurement of near bed cohesive sediment processes. HR Wallingford, Report SR 262.

James A E, Williams D J A, Williams P R, 1987. Rheologica Acta 26(5), p437.

Kirby R and Parker W R, 1973. Fluid mud in the Severn estuary and the Bristol Channel and its relevance to pollution studies. Inst. of Chem. Engrs. Annual Symp. on Estuarine and coastal pollution. Exeter.

Krishnappen B G, 1991. Modelling of cohesive sediment transport. International Symposium on the Transport of suspended sediments and its mathematical modelling, Florence.

Krone R B, 1962. Flume Studies of the Transport of Sediment in Estuarial Shoaling Processes, Final Report. Hydraulic Engineering and Sanitary Engineering Research Laboratory, University of California, Berkeley (CA).

Krone R B, 1972. A Field Study of Flocculation as a Factor in Esturial Shoaling processes, U.S Army Corps of Engineering, Comm. Tidal Hydraulics, Technical Bulletin, No 19.

Kusuda T, Umita T, Koga K, Yorozu H and Awaya Y, 1982. Depositional process of fine sediments, Wat. Sci. Tech. Vol. 14, Capetown, pp175-184.

Harleman D, 1961. Stratified Flow, in Handbook of Fluid Dynamics, ed. V Streeter, McGraw Hill, New York, USA.

HR Wallingford, 1989. Grangemouth mud properties. Report SR 197.

HR Wallingford, 1991. Fluid mud in estuaries: Final report to ETSU. Report EX 2392.

James A E, and Williams D J A, 1982. Flocculation and Rheology of Kaolinite/Quartz Suspensions Rheol. Acta 21, 176-183.

Jones T E R, and Golden K, 1990. Rheological Behaviour of River Parrett Fluid Mud. Report for Hydraulics Research Ltd.

Maa P T and Mehta A J, 1985. Considerations on Bed Response on Wave Resuspension of Muds, Paper Presented at the Symposium on Circulation Patterns in Estuaries, Virginia Institute of Marine Science, Gloucester Point, Virginia.

Mehta A J, 1988. Laboratory studies on cohesive sediment deposition and erosion , in Physical Processes in Estuaries, eds. Dronkers, van Leussen. Springer-Verlag, New York.

Mehta A J, Lott J W, 1987. Sorting of fine sediment during deposition. Coastal sediments, Vol 1, Proc. of conf. on advances in understanding of coastal sediment processes, New Orleans.

Mehta A J and Partheniades E, 1973. Depositional Behaviour of Cohesive Sediments, Technical Report No 16, Coastal and Oceanographic Engineering Laboratory, University of Florida, Gainesville (FL).

Migniot C, 1968. A study of the physical properties of various very fine sediments and their behaviour under hydrodynamic action, La Houille Blanche, 23, 7, (59-620)

O'Brien J S, and Julien P Y, 1986. Rheology of Non-Newtonian Fine Sediment Mixtures, Aerodynamics/Fluid Mechanics/Hydraulics, 988-997.

O'Brien J S, and Julien P Y, 1988. Laboratory Analysis of Mudflow Properties. Journal of Hydraulic Engineering (American Society of Civil Engineers), vl 114, No 8, 877-887.

Ockenden M C, Williamson H J, 1992. Estuarine sediments -near-bed processes: new modelling techniques for cohesive sediments. HR Wallingford, Report SR 299.

Odd N V M and Owen M W, 1972. A two-layer model of mud transport in the Thames estuary. Proc. ICE Supplement (iv). Paper 7517S.

Owen M W, 1971. The effect of turbulence on the settling velocities of silt flocs, Proc. Int. Association for Hydraulic Research, 14th Conference, Paris.

Partheniades E, 1962. A study of erosion and deposition of cohesive sediment in salt water. PhD Thesis, University of California.

Partheniades E, Cross R H and Ayora A, 1968. Further results on the deposition of cohesive sediments, Second Conference on Coastal Engineering Vol 1, Ch 47 London, September 1968.

Partheniades E, Kennedy J F, Etter R J and Hoyer R P, 1966. Investigations of the depositional behaviour of fine cohesive sediments in an annular rotating channel, Hydrodynamics Laboratory Report No 96.

Postma H, 1962. Sediment, in Demerara coastal Investigation : Delft, Netherlands, Hydrodynamics Laboratory, pp 105-164.

Puls W and Kuehl H, 1986. Field measurements of the settling velocity of estuarine flocs. Third International Symposium on River Sedimentation, Jackson, Mississippi, USA. March 1986.

Soulsby, R L, 1991. Private communication

Soulsby R L and Humphrey J D, 1989. Field observations of wave-current interaction at the sea bed. Proceedings of NATO Advanced Workshop on Water Wave Kinematics, ed. A Torum, Molde, Norway. Kluwer Academic Pub. BV. Dordrecht, Netherlands.

Soulsby R L and Smallman J V, 1986. A direct method of calculating bottom orbital velocity under waves, Hydraulics Research Ltd, Wallingford, UK. Report No SR 76, February 1986.

Stevenson J R and Burt T N, 1985. Further studies of the field settling velocities of Thames mud, Hydraulics Research Ltd, Wallingford, UK. Report SR 10.

van Leussen W, 1988. Aggregation of particles, settling velocity of mud flocs, a review. Proc. Int. Symp. Physical Processes in Estuaries, Springer-Verlag, pp347-403.

Verbeek H, Kuijper C, Cornelisse J M, Winterwerp J C, 1991. Deposition of graded natural muds in the Netherlands. Workshop on Nearshore and Estuarine Cohesive Sediment Transport, Florida, April 1991.

Verreet G, and Berlamont J, 1988. Rheology and Non-Newtonian Behaviour of Sea and Estuarine Mud. Encyclopedia of Fluid Mechanics, Vl 7, Cheremisimoff.

Wellershans S, 1981. Turbidity maximum and mud shoaling in the Weser estuary. Arch. Hydrobiol. 92. 2. 161-198.

Williams D J A, Williams P R, 1989. Journal of Coastal Research, Special Issue No 5, 165.

Williams D J A, Williams P R, 1990. in Microstructure of Fine-Grained Sediments, ed. Bennett, Bryant and Hulbert; Springer-Verlag, New York.

Williams P R, Williams D J A, 1989. Journal of Coastal Research, Special Issue No 5, 151.

Table

Table 5.1 Description of rheological Models (from Verreet and Berlamont, 1987) (see Figure 5.1)

Model	Curve	Equations	Material type
NEWTONIAN	1	$\tau = \eta \frac{du}{dz}$	dilute suspensions
		$\eta_r = 1 + 2.5\,\phi$	spherical particles
		$\eta_r = \exp[2.5\phi/(1 - k_1\phi)]$	
SHEAR THINNING (Pseudoplastic)	2	$\tau = m\,(\frac{du}{dz})^n \qquad n < 1$	flocculated clay slurries
		$\eta_a = m\,(\frac{du}{dz})^{n-1}$	
GENERALISED BINGHAM	3	$\tau = \tau_o + \eta_B(\frac{du}{dz})^n$ if $\lvert\tau\rvert \geq \tau_o$ with $\frac{du}{dz} = 0$ if $\lvert\tau\rvert < \tau_o$	
BINGHAM PLASTIC	3a	$\tau = \tau_{yB} + \eta\frac{du}{dz}$	
SHEAR THICKENING (Dilatant)	4	$\tau = k\,(\frac{du}{dz})^n \qquad n > 1$	concentrated deflocculated clay slurries
VISCO-ELASTIC (Voigt solid, Kelvin body)		$\tau = G\,\gamma + \mu\,\dot{\gamma}$	

Symbols

τ : shear stress
η : dynamic viscosity
η_s : dynamic viscosity of medium

$\eta_r = \frac{\eta}{\eta_s}$ = relative viscosity

$\eta_d = \frac{d\tau}{d\dot{\gamma}}$ = differential viscosity

$\eta_a = \frac{\tau}{\dot{\gamma}}$ = apparent viscosity

m : 'pseudoplastic viscosity'

τ_o = τ at $\dot{\gamma} = 0$
τ_{yB} : true Bingham plastic yield stress
τ_y : yield stress
τ_B : 'Bingham' yield stress
γ : shear deformation
$\dot{\gamma}$: shear rate
ϕ : solids volume fraction

n : flow index
k : shear-thickening analog of m
k_1 : constant
G : rigidity modulus or shear modulus

Figures

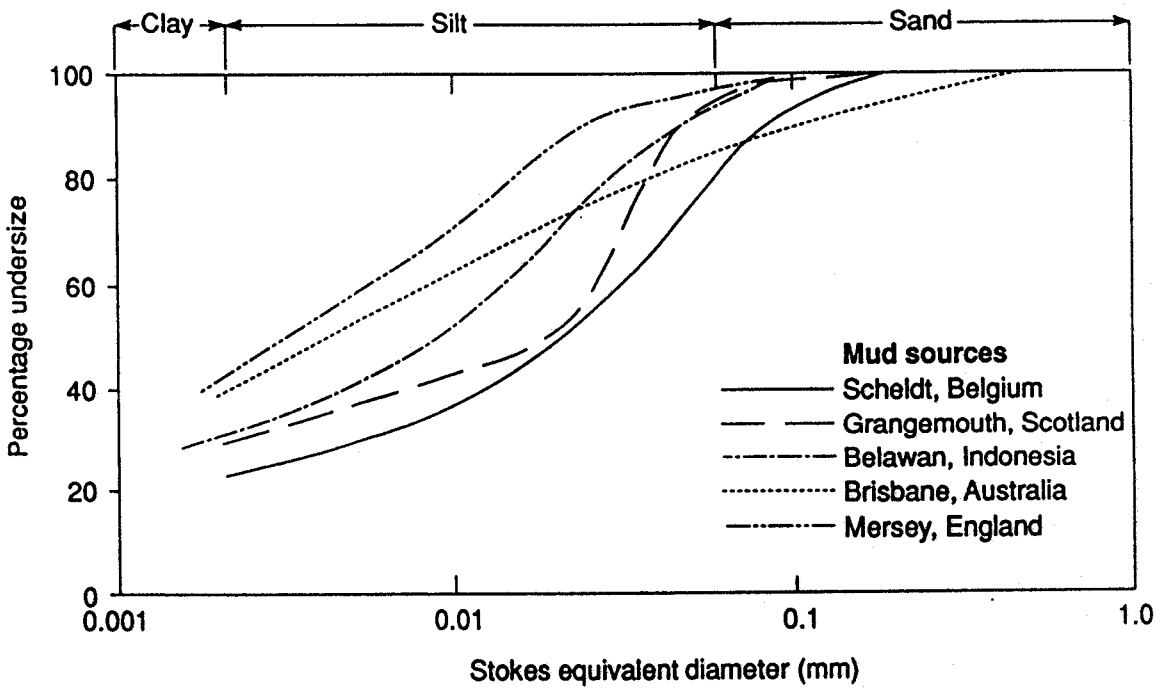

AD/F14/5-92/IB

Fig 1.1 Particle size distributions of cohesive sediment

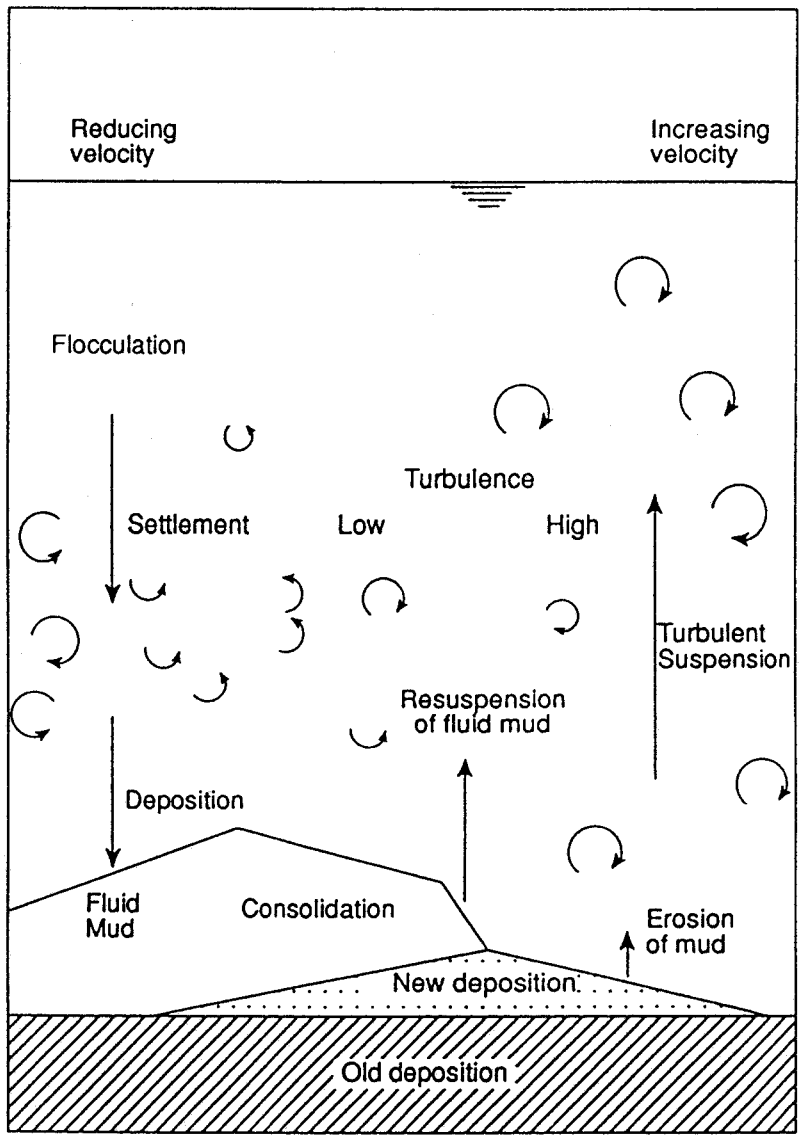

Figure 1.2 Schematic diagram illustrating four states of cohesive sediment during a tide

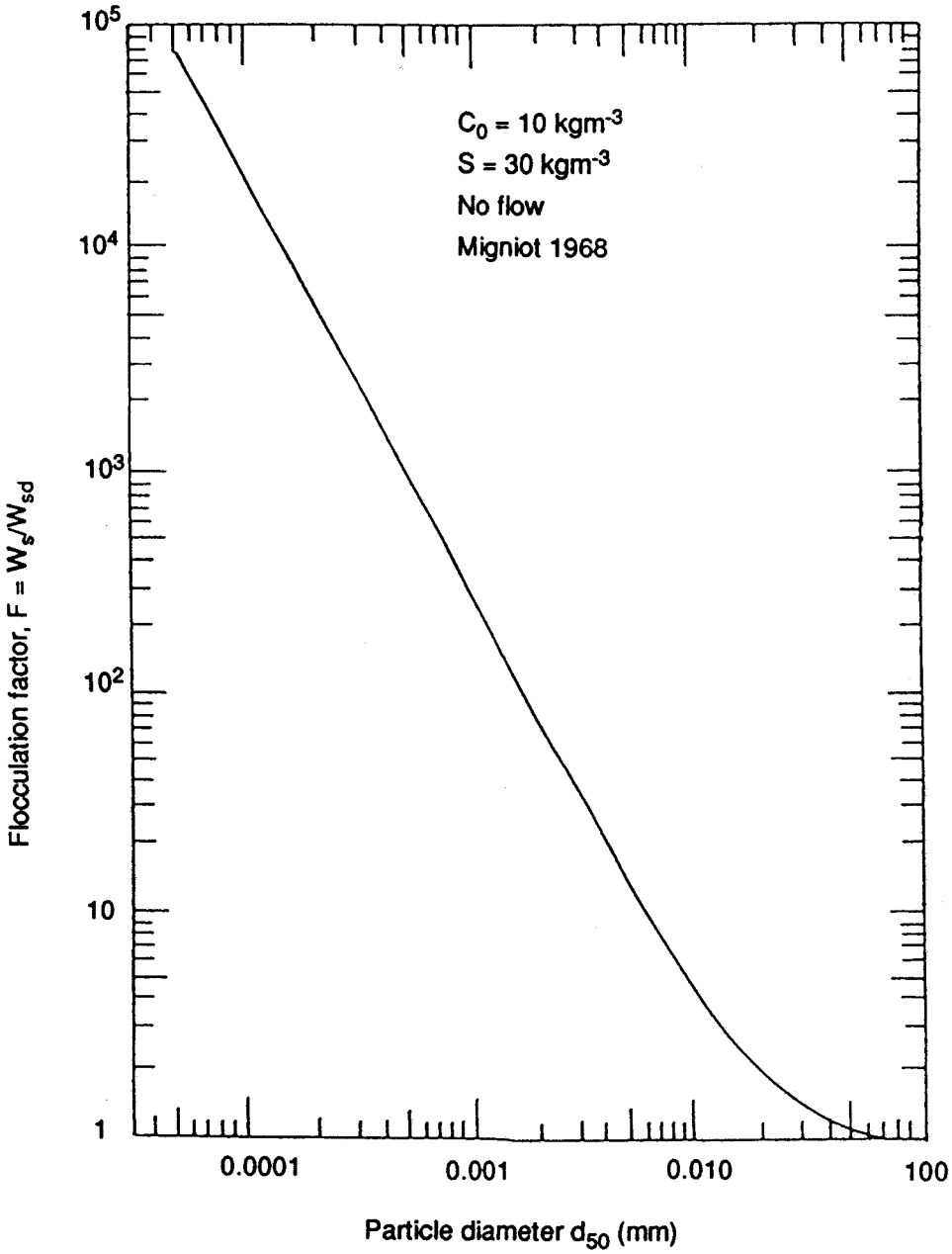

AD/F2.1/5-92/IB

Figure 2.1 Ratio of flocculated to chemically dispersed settling velocity of suspended cohesive sediment against average particle size

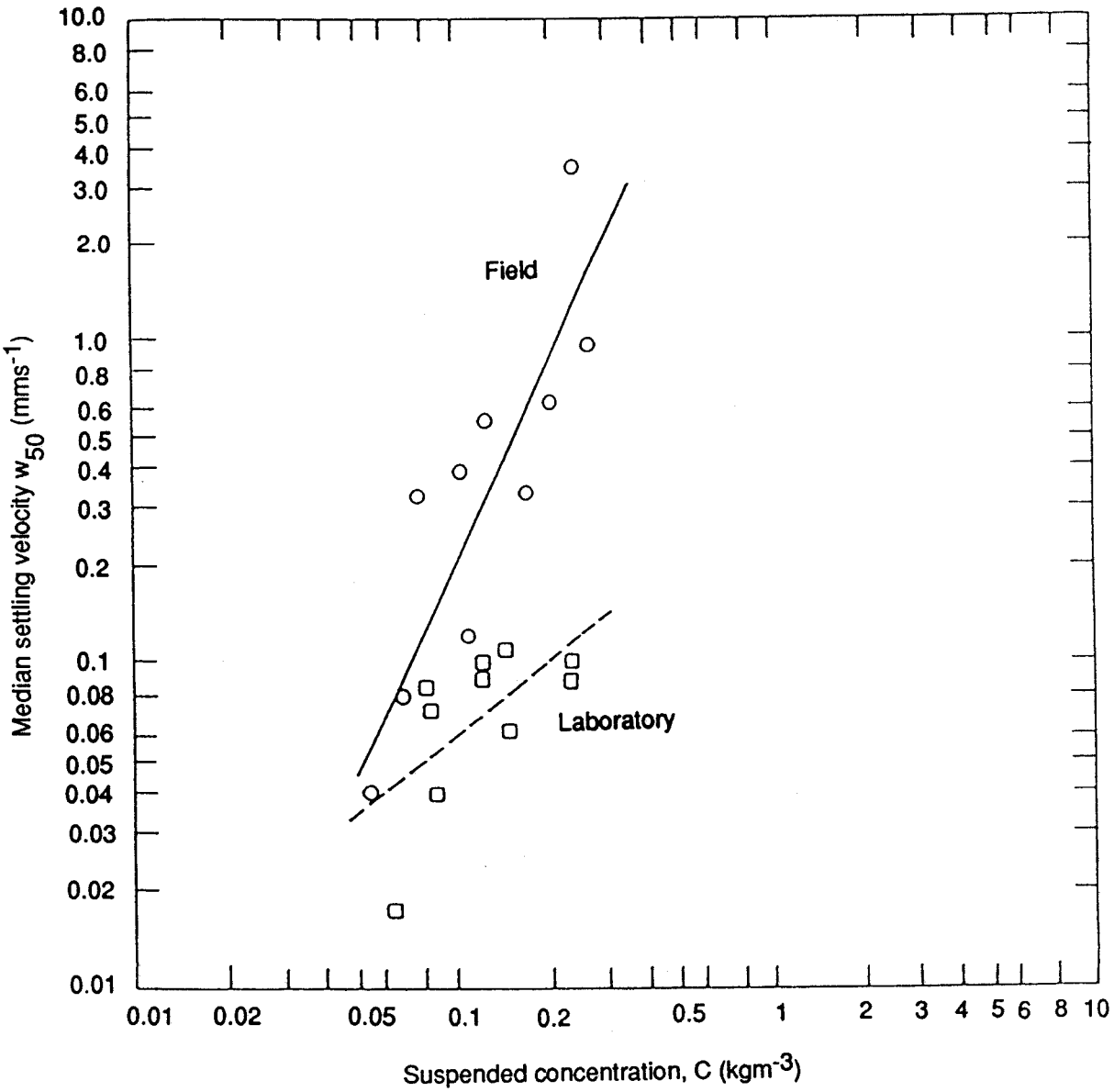

AD/F2.2/5-92/IB

Figure 2.2 Field and laboratory determined median settling velocity of suspended cohesive sediment against suspended sediment concentration

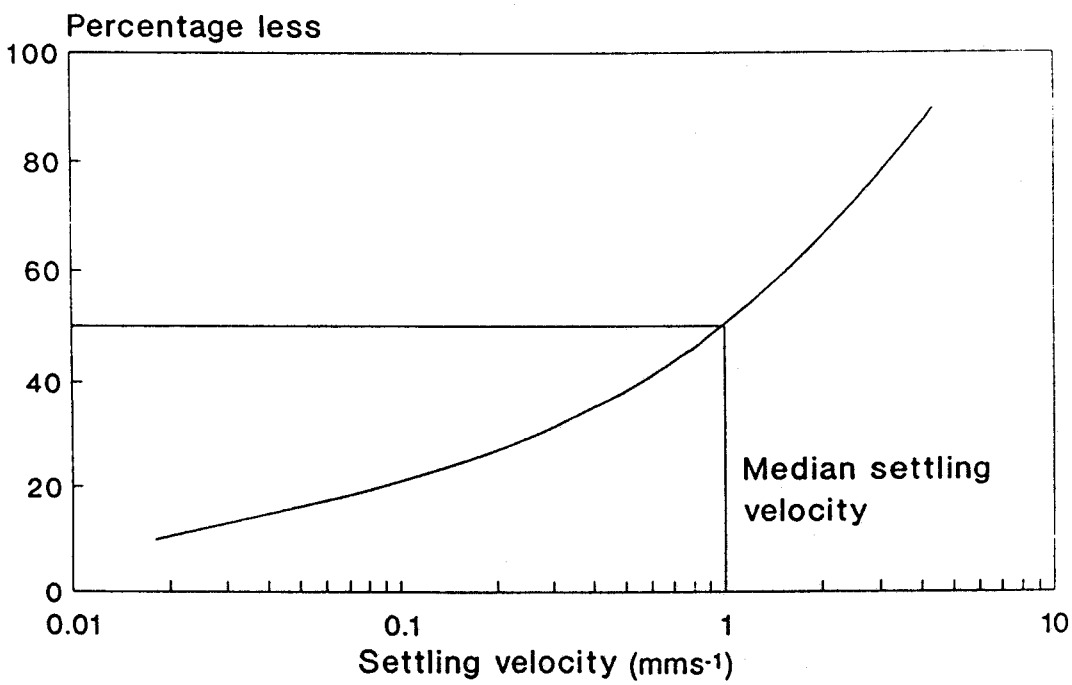

AD/F2.3/5-92/IB

Figure 2.3 Distribution of floc settling velocity of River Thames suspended cohesive sediment against cumulative weight

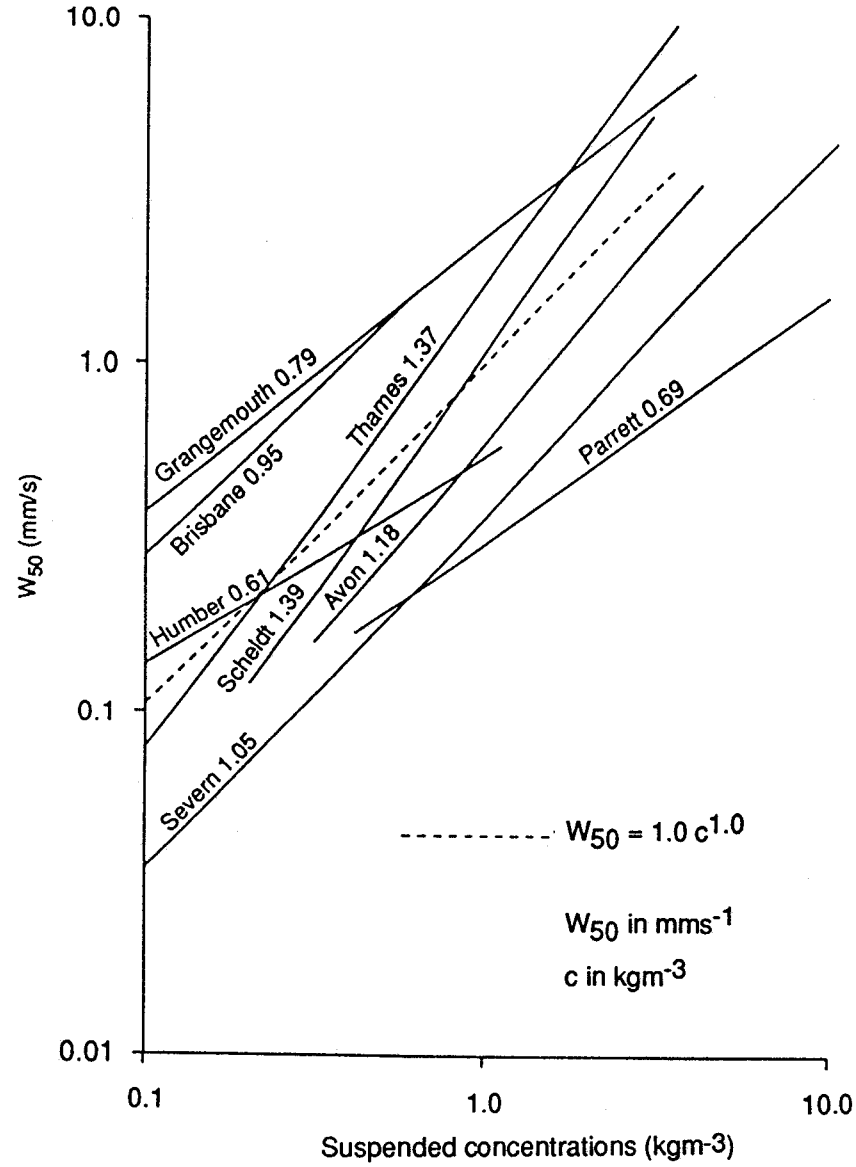

AD/F2.4/5-92/IB

Figure 2.4 Field determined median settling velocity of suspended cohesive sediment from different sites against suspended sediment concentration

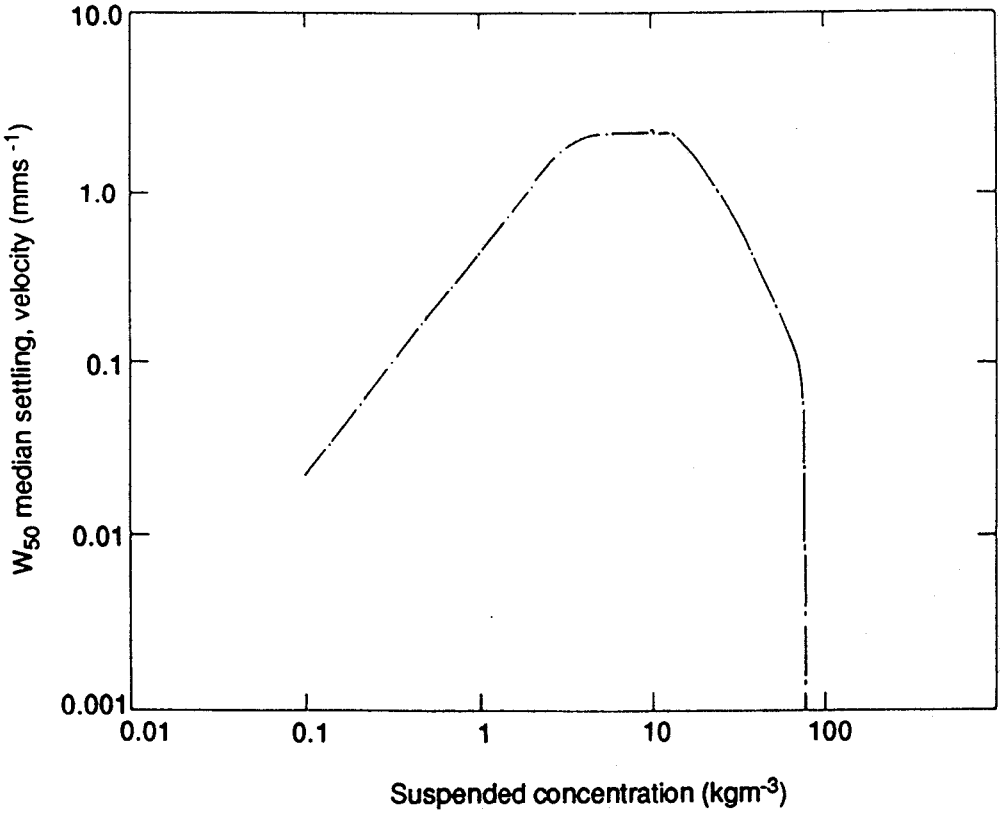

AD/F2.5/5-92/IB

Figure 2.5 Field determined median settling of Severn Estuary suspended cohesive sediment against suspended sediment concentration

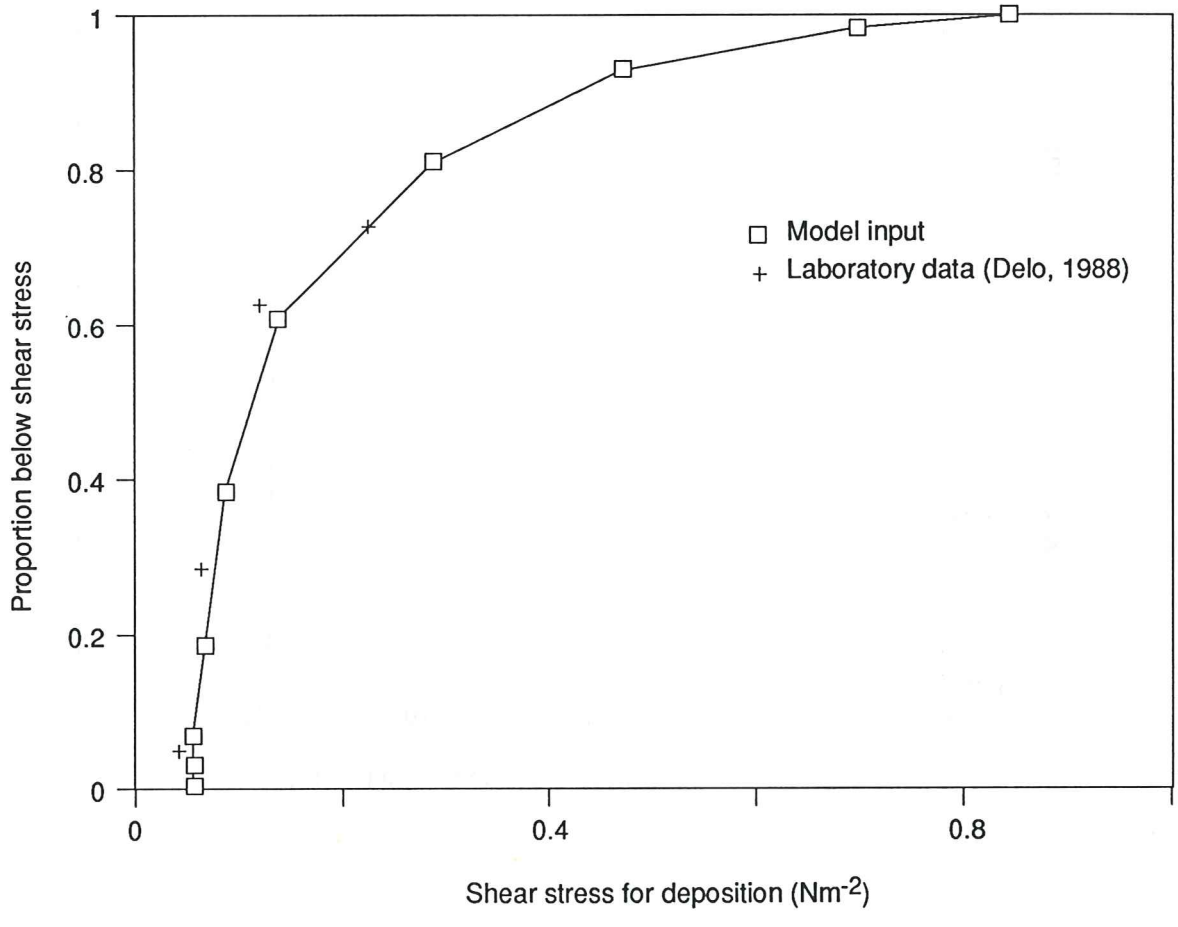

AD/F14/5-92/IB

Figure 2.6 Critical shear stress for deposition of cohesive sediment from laboratory deposition tests

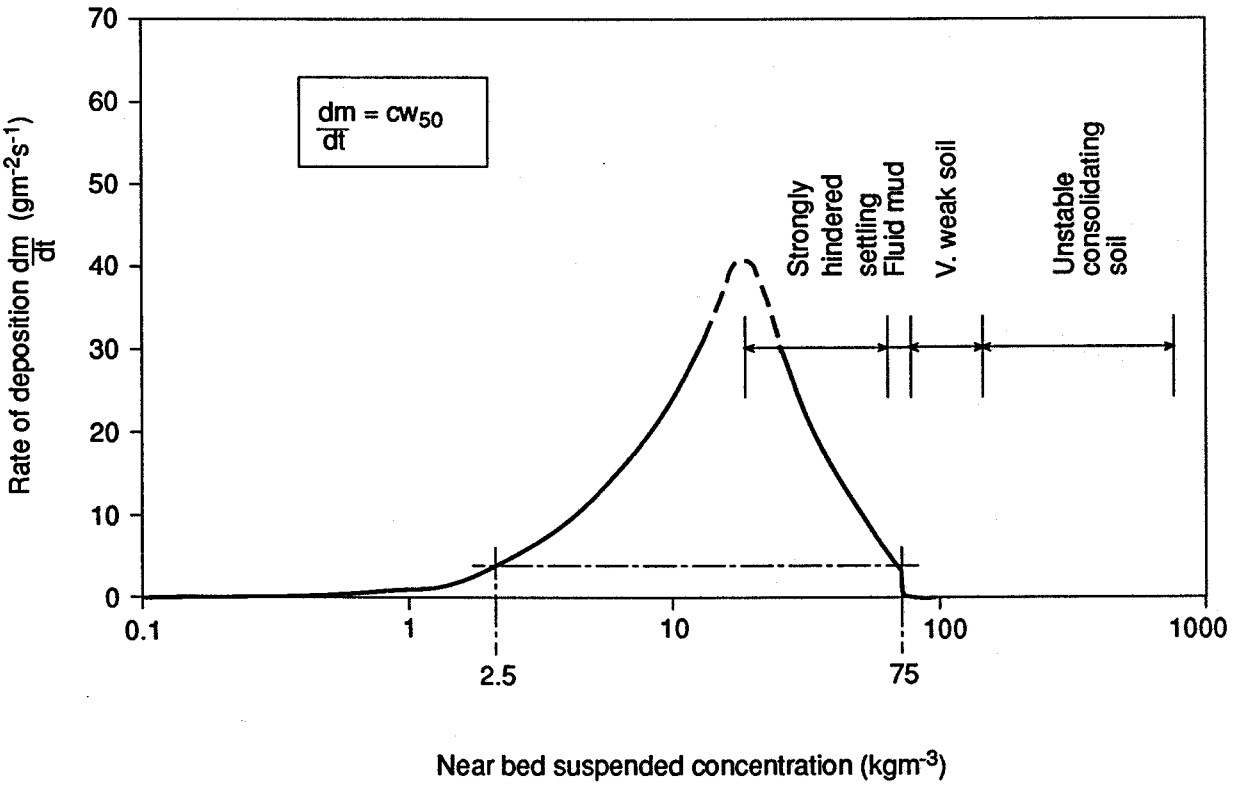

AD/2.7/6-92/IB

Figure 2.7 Rate of deposition of suspended cohesive sediment against near bed suspended concentration

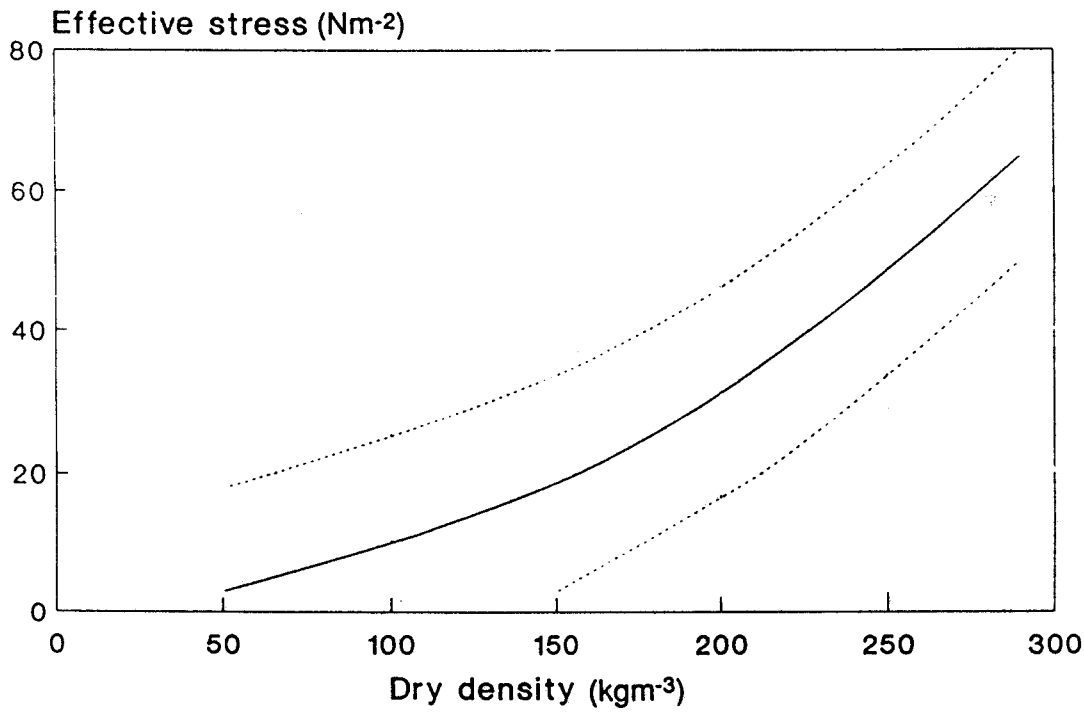

AD/F3.1/5-92/IB

Figure 3.1 Typical relationships from laboratory consolidation tests on cohesive sediment of effective stress at various times and depths below the surface against dry density

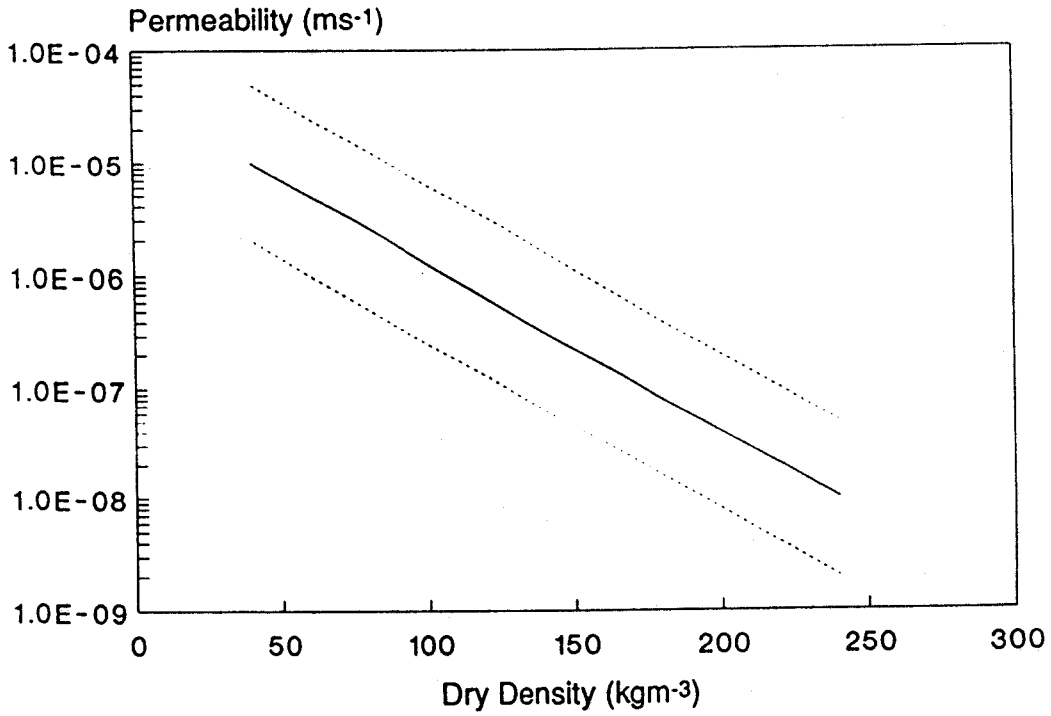

AD/F3.2/5-92/IB

Figure 3.2 Typical relationships from laboratory consolidation tests on cohesive sediment of permeability at various times and depths below the surface against dry density

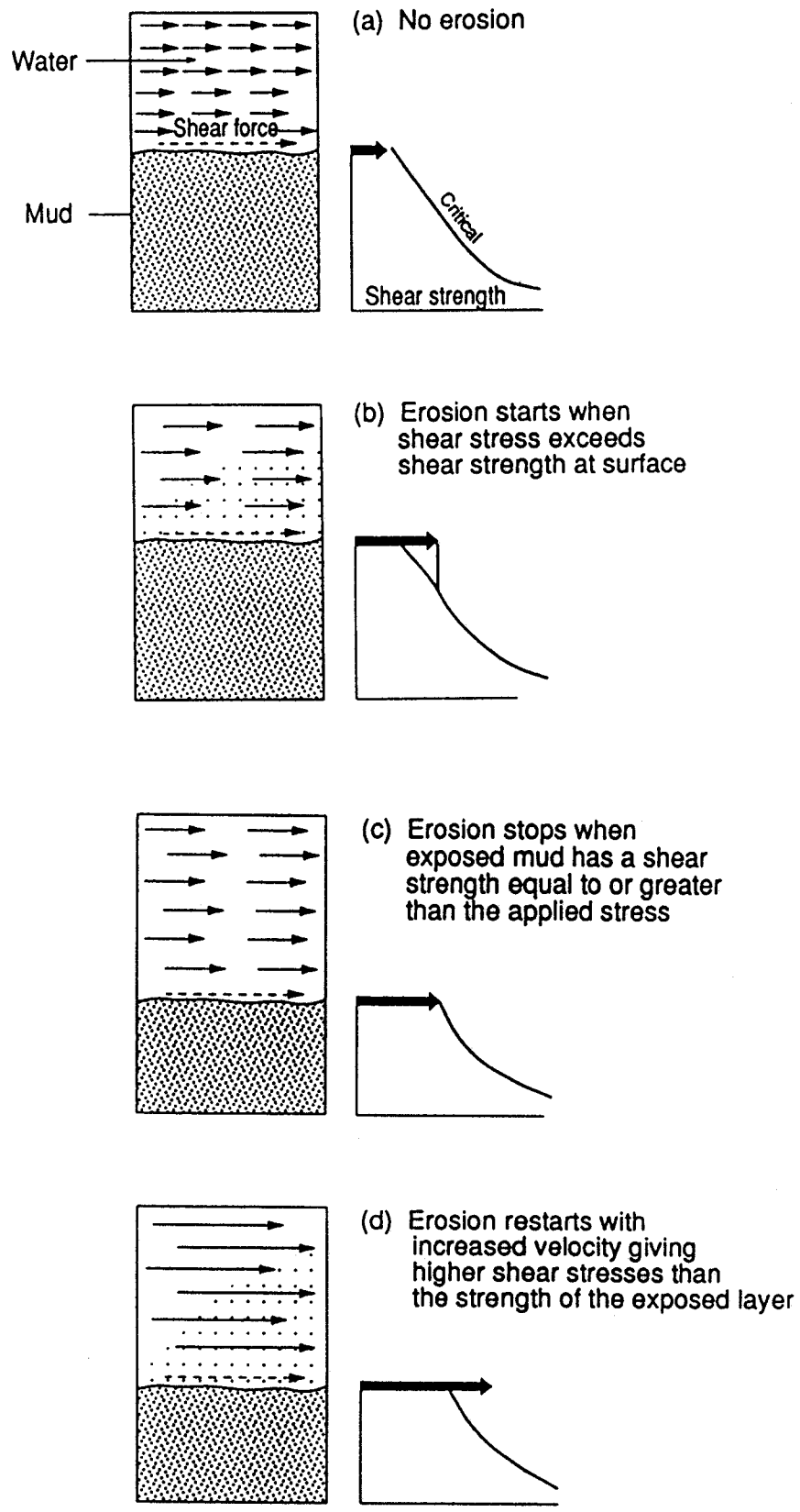

Figure 4.1 Schematic diagram illustrating the cohesive sediment erosion process

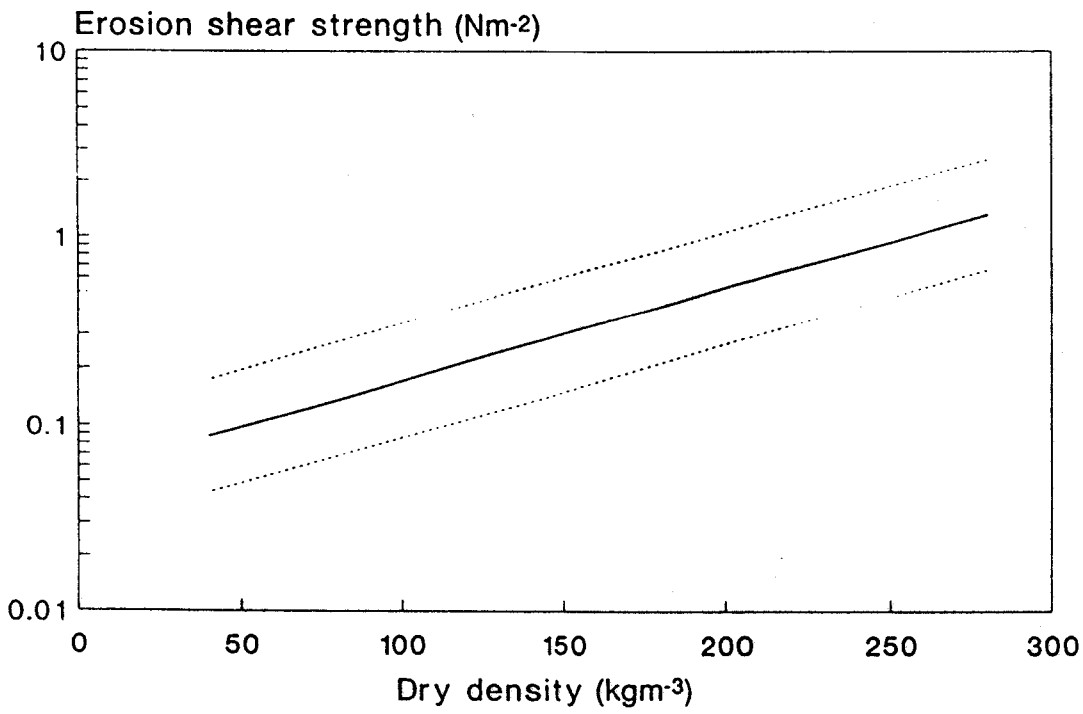

AD/F4.2/5-92/IB

Figure 4.2 Typical relationships from laboratory erosion tests on cohesive sediment of erosion shear strength against dry density

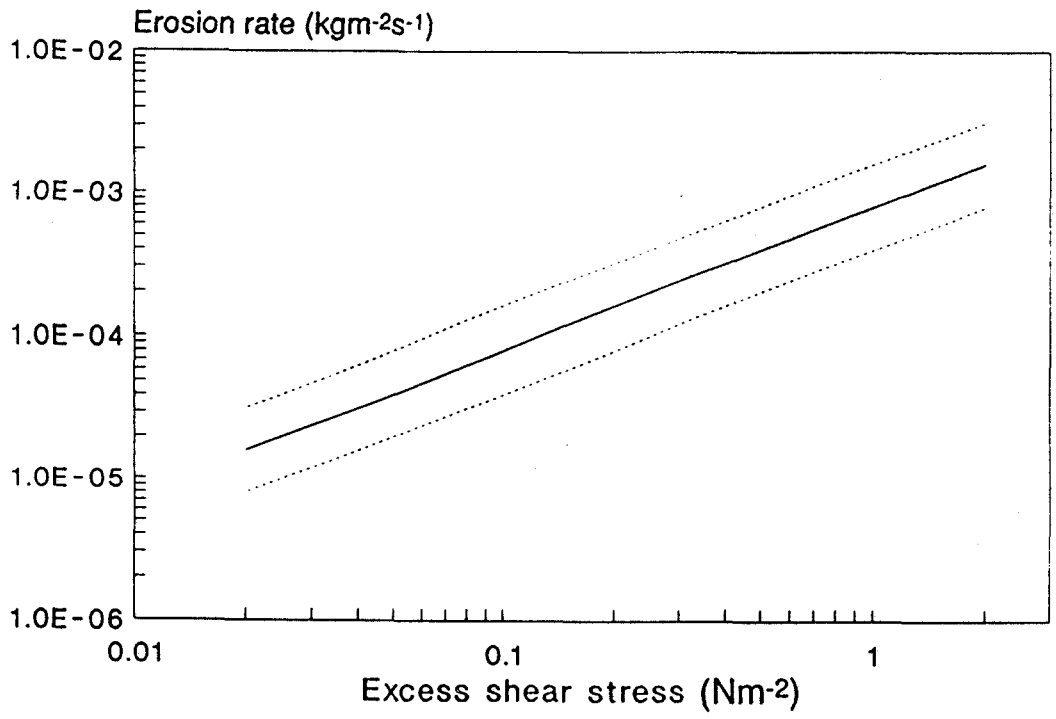

AD/F4.3/5-92/IB

Figure 4.3 Typical relationships from laboratory erosion tests on cohesive sediment of erosion rate against excess shear stress

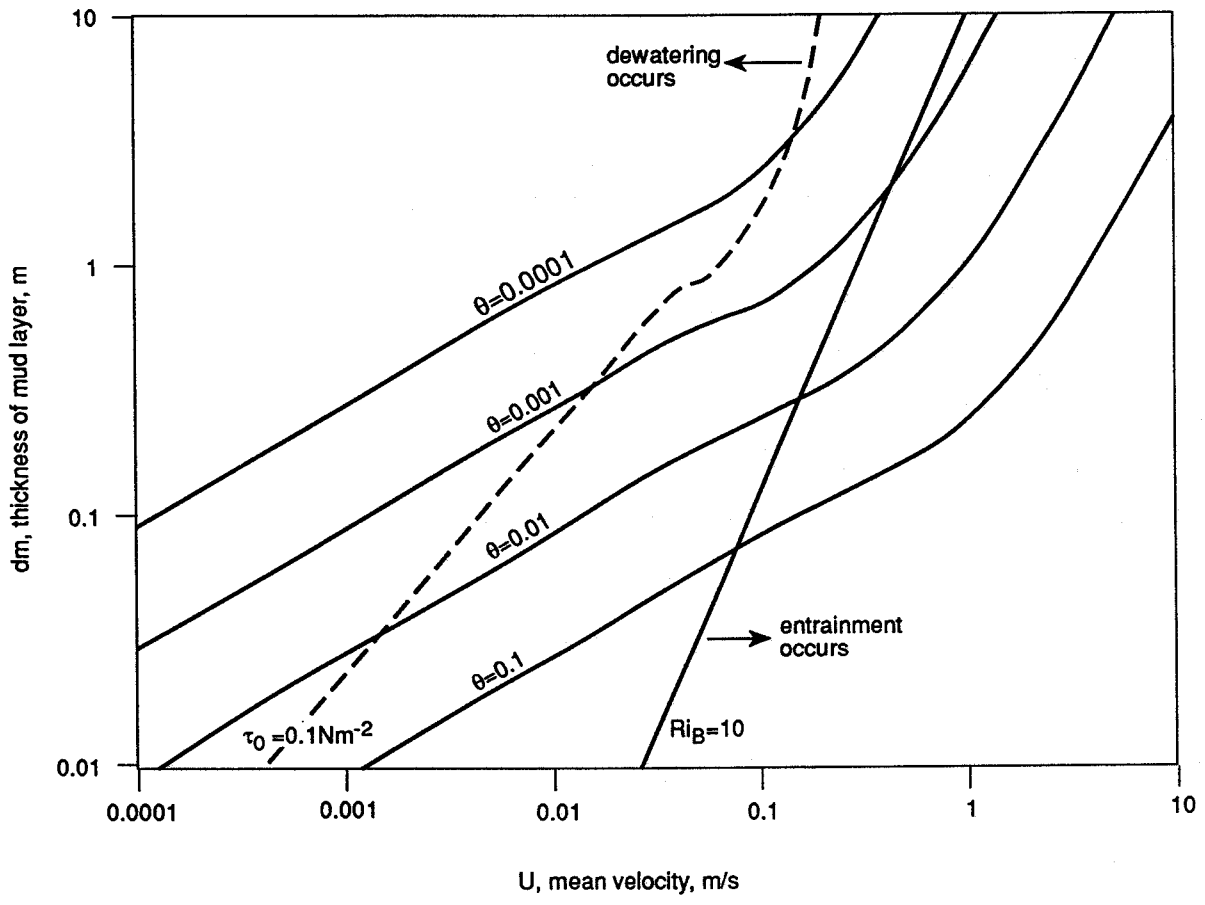

AD/F14/5-92/IB

Figure 4.4 Motion of fluid mud down a sloping bed in still water

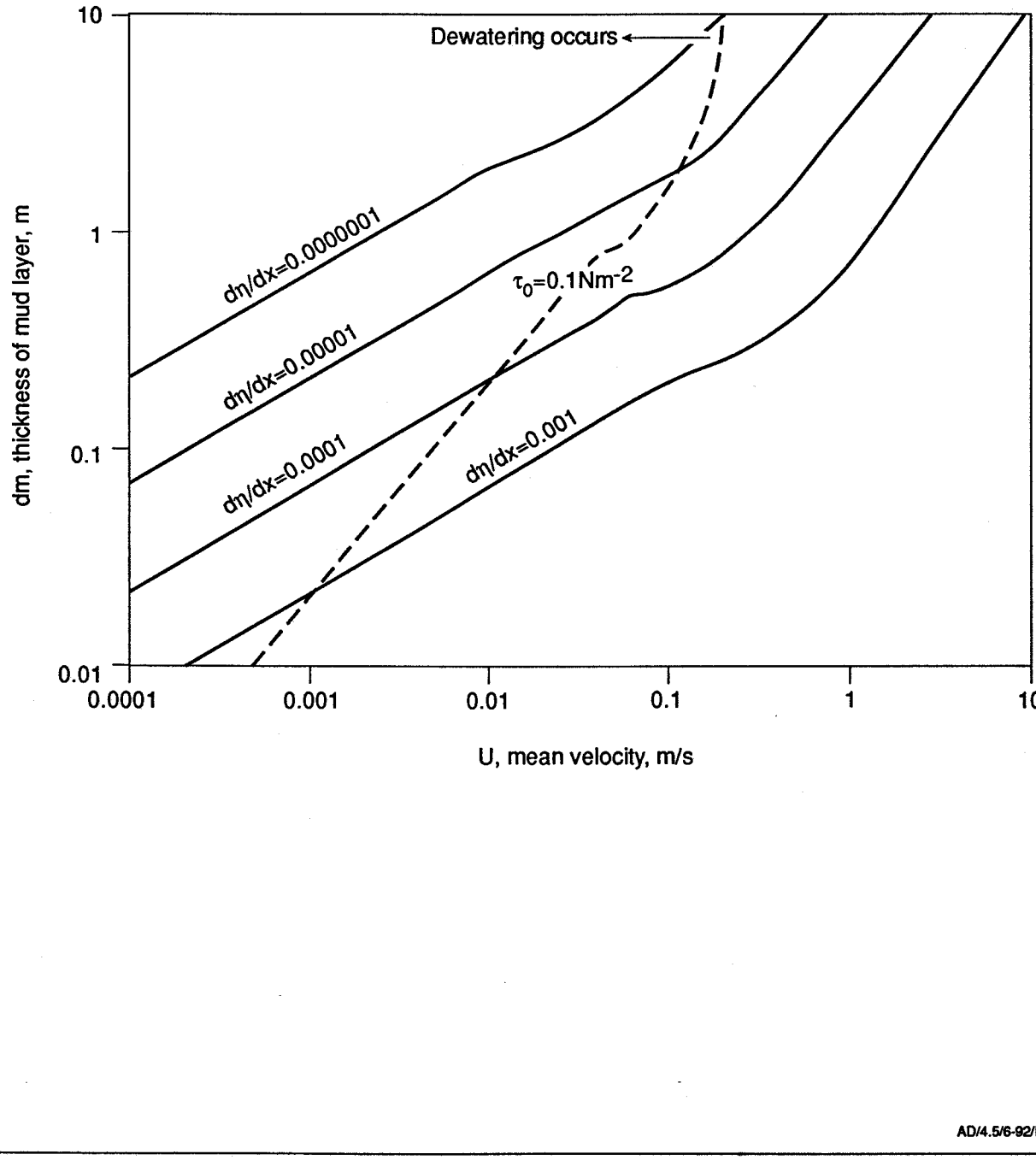

Figure 4.5 Motion of fluid mud under an applied water surface slope

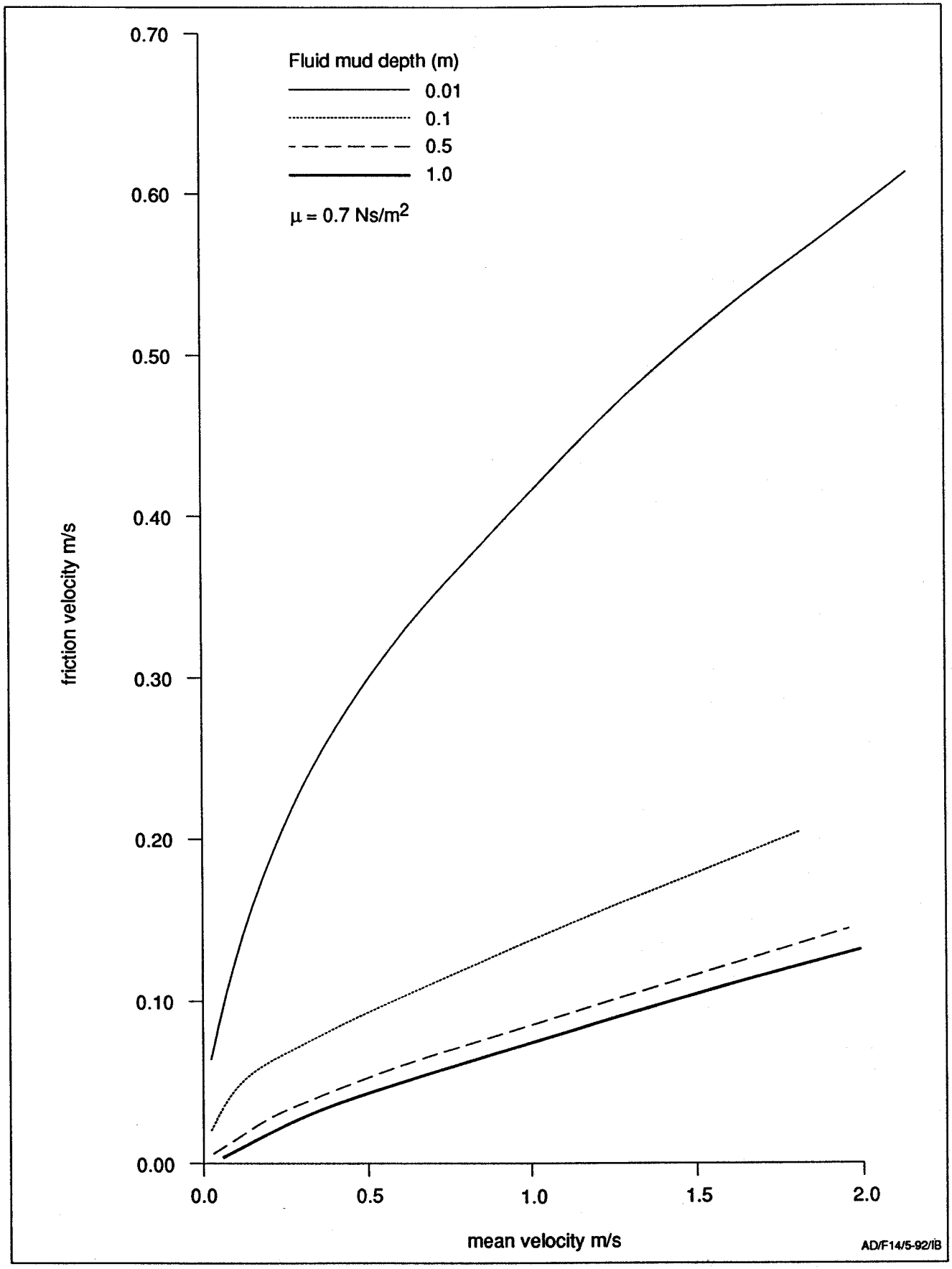

Figure 4.6 Friction velocity as a function of depth and mean velocity of a fluid mud layer

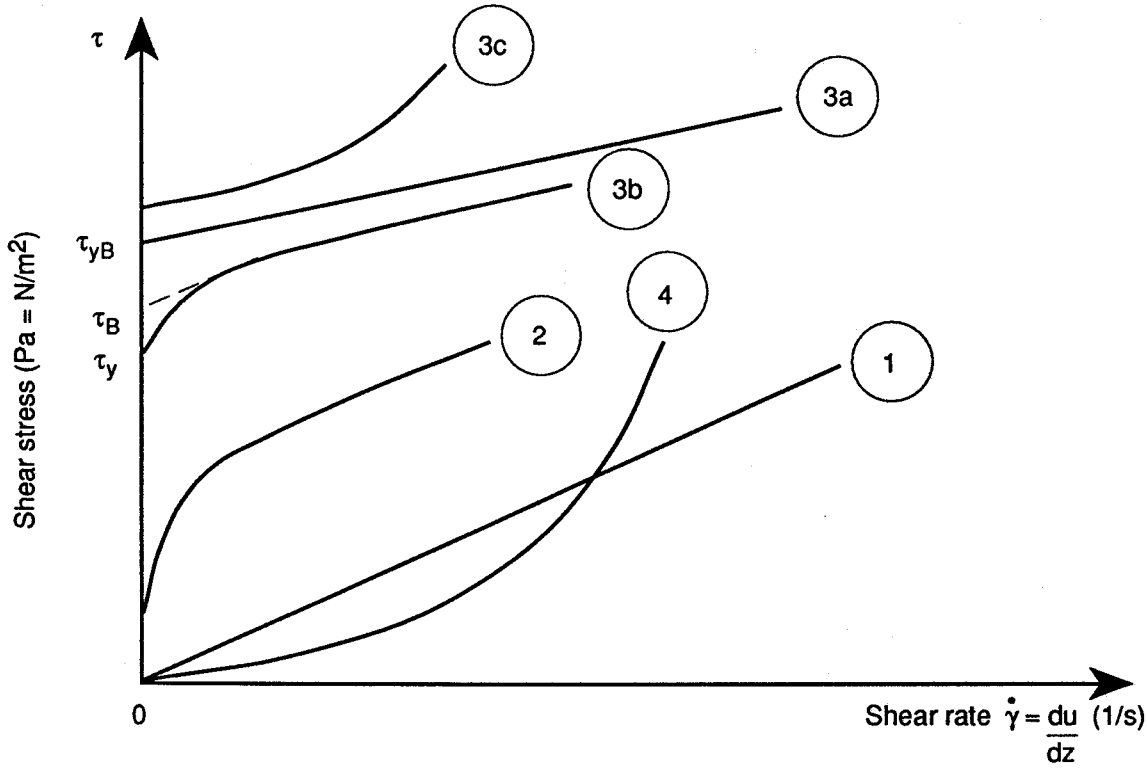

AD/F14/5-92/IB

Figure 5.1 Schematic representation of rheological models (after Verreet and Berlamont, 1987; see also Table 5.1)

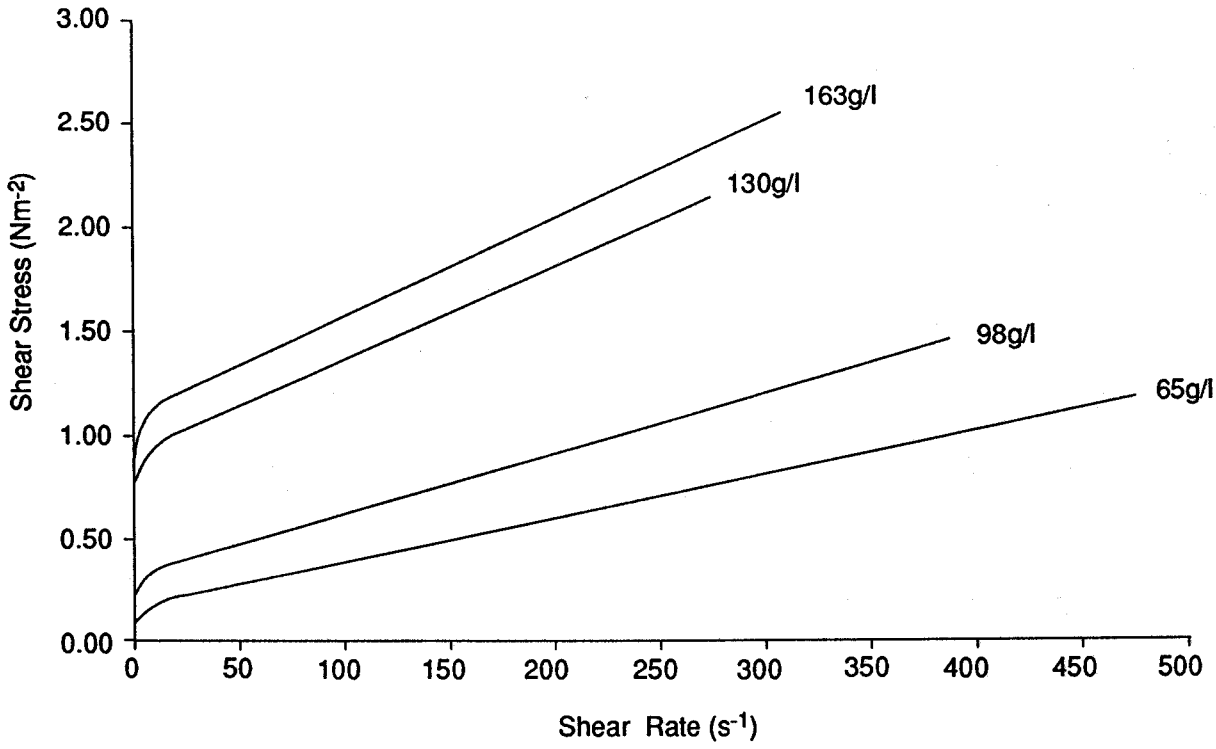

Figure 5.2 Shear stress/shear rate flow curves for different concentrations

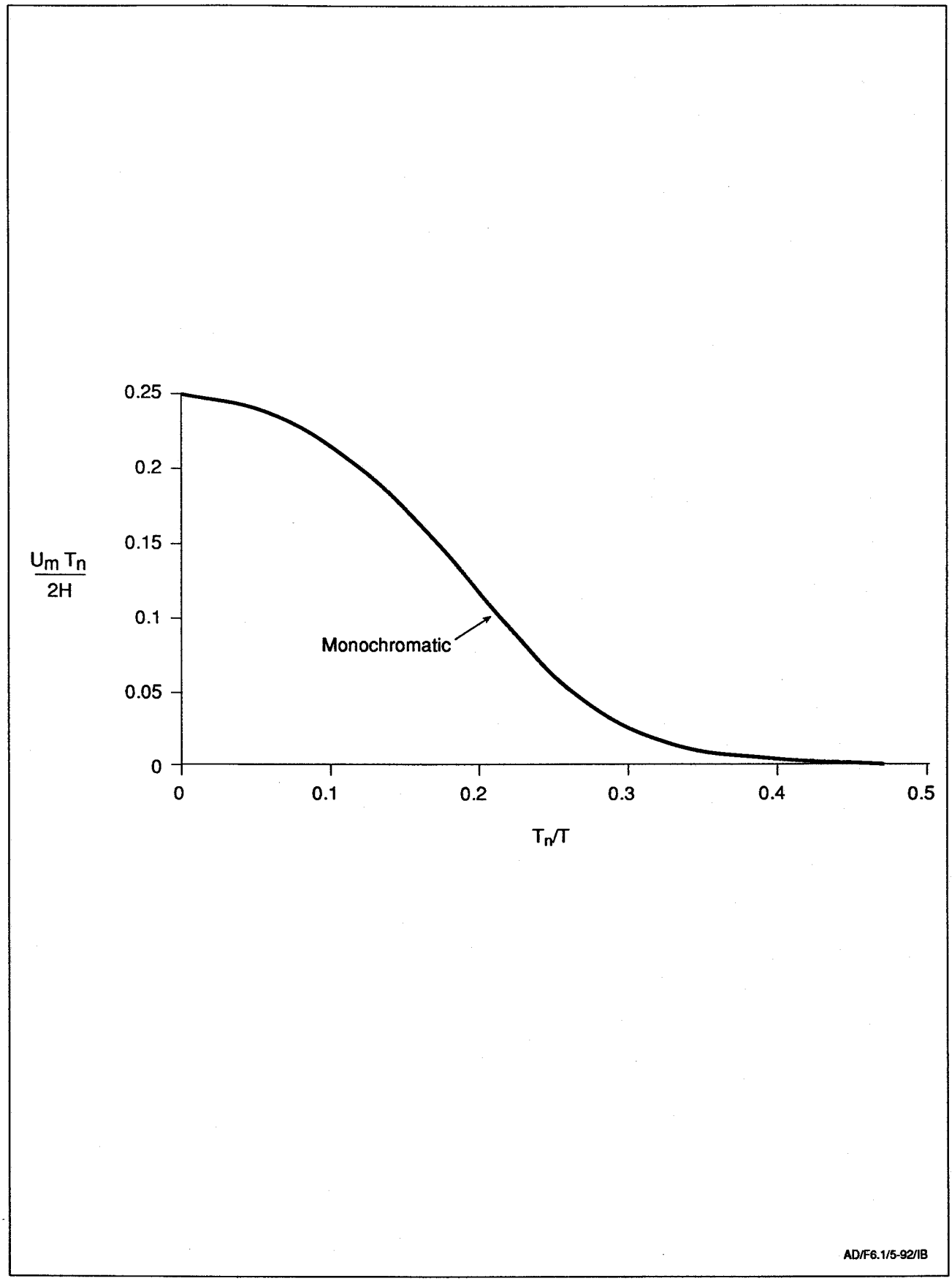

Figure 6.1 Bottom velocity for monochromatic waves ($U_m T_n/2H$ versus T_n/T) where $T_n = (h/g)^{1/2}$